Improvement of In Vitro Fertilization (IVF) Technology through Microfluidics

by

Yunseok Heo

A dissertation submitted in partial fulfillment
of the requirements for the degree of
Doctor of Philosophy
(Biomedical Engineering)
in The University of Michigan
2008

Doctoral Committee:

Associate Professor Shuichi Takayama, Chair
Professor Robert T. Kennedy
Associate Professor Joseph L. Bull
Associate Professor Gary D. Smith

DEDICATION

This dissertation is dedicated to my family.

My mother, Oak Soon Lee and late father, Dae Chul Heo

have positively encouraged me to always expect nothing but the best from myself.

A special feeling of gratitude

to my loving wife, Young Joo Cho for devotion, encouragement.

to my lovely, precious son, Joshua Jihoo Heo for dream, motivation and hope.

My brother, Yun Young and sisters, Ji Sook, Ji Yeon and Ji Eun

have never left my side and are very special.

ACKNOWLEDGEMENTS

I would like to gratefully acknowledge my advisor, Dr. Shuichi Takayama, for his continued guidance throughout my graduate career. Dr. Takayama represents to me the model brilliant scientist who continually searches for new challenges, pushes boundaries, and is thoroughly committed to the development of his students. I am very thankful to have been one of his students. I would also like to acknowledge the members of my dissertation committee: Drs. Robert T. Kennedy, Joseph Bull, and Gary D. Smith. They have been my professor. All of whom along with Dr. Takayama are my role models as scientists.

I would like to graciously acknowledge the people who are co-authors in publications with me that comprise this dissertation: Lourdes M. Cabrera, Dr. Nobuyuki Futai, Dr. Charles L. Bormann, Christopher T. Shah, Dr. Jonathan W. Song, Dr. Yi-Chung Tung. I would also like to thank the staff of the BME department, particularly Mayte Brown. Finally, I would like to thank all the members of the Takayama lab and the friends I have made while here at the University of Michigan. During my graduate studies, I have learned and enjoyed myself more than any other time in my life. The people I have met during my time at Michigan are the reasons why.

TABLE OF CONTENTS

LIST OF FIGURES

Figure

ABSTRACT

Despite advances in *in vitro* manipulation of pre-implantation embryos, there is still a lag in the quality of embryos produced *in vitro* leading to lower pregnancy rates compared to embryos produced *in vivo*. Reducing the incidence of high-order multiple pregnancies while maintaining the overall *in vitro* fertilization (IVF) success rate is a holy grail of human IVF and would be greatly assisted by the ability to produce and identify the highest quality embryos. A promising new technology, microfluidics, does exist and is becoming increasingly studied. A challenge of studying embryo on microfluidic device is that preimplantation mouse embryos are highly sensitive cells and their development is affected greatly by osmolality shifts as will occur in devices with thin poly(dimethylsiloxane) (PDMS) membranes even in typical humidified cell culture incubators. Here we characterized and resolved evaporation mediated osmolity shifts that constrained microfluidic cell culture in Poly(dimethylsiloxane) devices. Next, we developed a dynamic microfunnel embryo culture system would enhance outcomes by better mimicking the fluid mechanical stimulation and chemical agitation embryos experience *in vivo* from ciliary currents and oviductal contractions. Using a mouse embryo model, average cell counts for blastocysts after 96 hours of culture in dynamic microfunnel conditions increased 70% over that of conventional static cultures. Importantly, the dynamic microfunnel cultures significantly improved embryo implantation and ongoing pregnancy rates over static culture to a level that approached

that of in utero-derived preimplantation embryos. Lastly, we reported a new computerized microfluidic real time embryo culture and assay device that can perform automated periodic analyses of embryo metabolism over 24 hrs. Biochemical methods for embryo analysis based on measurement of metabolic rates do exist, but are not practical for clinical use because of difficulties in manipulating precise amounts of sample and reagents at the sub-microliter scale. The convenient, non-vasive, reliable, and automated nature of these assays open the way for development of practical single embryo biochemical analysis systems. Collectively, these results confirm that microfluidic technology can be used to properly mimic a broad range of the embryo environments seen in physiology and to assess embryo viability for in vitro fertilization clinics.

CHAPTER I

Introduction

Despite advances in *in vitro* manipulation of pre-implantation embryos, there is still a lag in the quality of embryos produced *in vitro* leading to lower pregnancy rates compared to embryos produced *in vivo*. Since the first *in vitro* development of fertilized mouse ova was cultured on a blood clot with an extract of oviduct tissue in 1941, extensive research has been undertaken in order to improve the culture media used by modifying standard components, the energy or nitrogen sources, or by supplementing them with other substances that are believed to improve blastocyst development. Although optimizing media conditions has become an important approach for enhancing the success rate for treatment of human infertility, currently used *in vitro* conditions fail to mimic the *in vivo* environment. Mammalian fertilization and embryo development are assisted by the coordinated activity of motile spermatozoa, muscular contractions of the uterus and oviduct, as well as ciliary beating. These structures generate forces that drive fluid motion *in vivo*[1]. These environmental factors of the physiological fertilization process cannot be fully recapitulated by formulation of media alone. A better understanding of dynamic *in vivo* reproductive processes combined with advances in microfluidic cell handling have recently converged to allow further enhancements in embryo development and pregnancy rates by enhancement of the culture hardware. In this chapter, we review the basic micro-structural and fluid mechanical aspects of the reproductive processes *in vivo* and provide examples of how

microfluidic devices have been able to recapitulate an aspect of the physiological environment *in vitro* to enhance assisted reproduction.

Spermatogenesis, sperm migration and oogenesis

Spermatogenesis is a highly ordered multi-step process involving multiple cellular divisions and complex differentiation cascades through which spermatogonial stem cells give rise to mature spermatozoa[2]. In the human, the entire process of spermatogenesis takes a period of about 70 days[3] and mature sperm cells consist of a head (~3μm in diameter and ~5μm in length) and a tail (~ 1.5 μm in diameter and ~ 50μm in length)[4]. In humans, up to 300 million spermatozoa suspended in 3 to 5ml of seminal fluid are deposited in the vagina at ejaculation. Physiologically, there are several selection steps that sperm must pass through before reaching the oocyte. The endocervix presents approximately 100 crypts from which mucus flows toward the external os. During coitus, semen comes in contact with mucus that fills the external os of the uterine cervix. The cervical mucus serves as a first barrier allowing easier passage of sperm with superior morphology[5,6]. Further drastic reductions in numbers occur across the cervix in species with vaginal insemination and at the uterotubal junction (UTJ) and ampullary-isthmic junction (AIJ) (Figure I.1). Successful conception requires that a mature sperm arrive at the site of fertilization, the ampullar region of the fallopian tube (oviduct).

Sperm cells with the tail flagellates are propelled at about 1~3 mm/min in humans by whipping in an elliptical cone[7]. Sperm migration occurs in two phases, at least in some species: a rapid phase whereby sperm reach the upper segments of the oviduct within minutes

from insemination and a slow phase whereby spermatozoa reach the oviduct over several hours[8]. Human sperm may reach the upper segments of the oviduct within minutes from insemination[9]. This speed of passage far exceeds the swimming velocity of sperms and is explained by the muscular contractions of the uterus[10], which is also supported by the fact that even some dead sperm also undergo rapid transport following artificial insemination[8].

Oogenesis begins with formation of primordial germs cells (PGCs) and encompasses a series of cellular transformation, from PGCs to oogonia (fetus), from oogonia to oocytes (fetus), and from oocytes to eggs (adult)[2]. In 8-day mouse embryos, PGCs (~12μm) are found in the yolk sac endoderm and in that region of the allantois arising from the primitive streak. The oocyte grows from a diameter of ~12μm (volume ~0.9 pl) to final diameter of ~12μm (volume ~ 270 pl), not including the zona pellucida (ZP). Each oocyte is contained within a cellular follicle (~17μm) that grow concomitantly with the oocyte, from a single layer of a few flattened cells to three layers of cuboidal granulosa cells (~900 cells; ~125μm follicle) by the time the oocyte has completed its growth. During a period of several days, while the oocyte remains a constant size, the follicular cells undergo rapid division, increasing to more than 50,000 cells and result in an antral or graafian follicle greater than 600μm in diameter.

This thesis does not directly work on mimicking the processes of spermatogenesis, sperm migration and oogenesis but the topic is briefly included to point out the challenges and opportunities in filling the gap between existing *in vitro* gamete handling and the *in vivo* process. There are many opportunities to close the gap using microfluidic technology in multiple steps from the early stage in gamete to the preimplantation embryo stage. I specifically worked on preimplantation embryo culture and selection among the multiple

procedures. In the next section, the microenvironment for early stage embryo development in the oviduct will be described in detail for better understanding of what factors are most important to mimic the physiological microenvironment.

Microenvironment and embryo transport in the oviduct

In fertilization *in vivo*, the fallopian tube or oviduct plays an essential role in gamete transport, fertilization and the early development of the embryo. In the order from ovary to uterus, oviduct commonly consists of five sections: Fimbria, Ampulla, Ampullary-isthmic junction (AIJ), Isthmus, Isthmus-uterotubal junction (UTJ). Embryos developing from zygotes to blastocysts *in vivo*, travel slowly through the isthmus in the oviduct toward the uterus in a few days under dynamic activities in terms of mechanical and chemical factors. The oviductal musculature and the cilia have been considered as potential effectors of the movement. It has been reported that smooth muscle contraction plays a major role in transport of the early stage of embryo from isthmus to the uterus in a few days[11] while oocytes or zygotes is transported into the oviductal ampulla and rapidly toward the ampullary-isthmic junction by ciliary action[12]. Since fertilized embryos spend most time in the isthmus before settling down in the uterus, smooth muscle contraction plays a major role in the dynamic conditions for the early stage embryo development, which is also strengthened by the fact that the isthmus of the oviduct is generally lined by far fewer ciliated cells than the ampulla[13] and possesses a thicker muscular tunic. In addition to embryo transport, the purpose of these segmental muscular contractions may be to stir tubal contents and ensure the mixing of gametes and embryos with tubal secretions[14]. Muscular activity of

the oviductal isthmus was recorded in intact awake rabbits. Mean frequencies during the time period of the isthmus was approximately 8.1contractions/min which is equivalent with 0.135 Hz[15]. Further studies on models of contraction showed that a sequence of contraction in the uterine direction (a pseudo-peristalic wave) will lead to positive ovum transport[16].

Important considerations for recapitulating the embryo microenvironment include the fluid dynamic properties dictating embryo transport and development and the hormones controlling these mechanical parameters. Quantification of these parameters will facilitate the development of accurate computer models for understanding the effects that particular mechanical and chemical cues have on embryo development and allow for the development of enhanced experiments for testing embryo development under more dynamic, realistic conditions. To this end, great efforts have been put forth to quantify the ciliary beating frequency (CBF) of the cilia that line the oviduct; various animal models and even human models have been used to quantify this parameter under different conditions. Using a laser Doppler flowmeter system to measure CBF in Rabbit cilia of the oviduct, Holloway and colleagues[17] found that the mean frequency was approximately 8.5 Hz at ambient temperature and 25 Hz at 36°C; furthermore, it was found that there was a linear relationship in this range between CBF and temperature. The media in which the oviducts were examined also proved to be of great significance. Lyons *et. al.*[18] determined that there were differences between CBF when human oviducts were bathed in peritoneal fluid and ovarian follicular fluid at room temperature, where the latter case exhibited a higher CBF (6.34 Hz compared to 5.24 Hz). Other chemical cues from the microenvironment appear to have a substantial influence upon the CBF; Mahmood *et. al.*[19] demonstrated that incubation of human fallopian tube epithelial cells with progesterone resulted in a suppression of CBF by

40-50%. The ultimate purpose of ciliary beating is for conveying embryos to particular areas of the fallopian tube. The range of CBF values mentioned previously translates to transport velocities ranging from 0.03 mm/s – 0.11 mm/s. Since the CBF is highly dependent on the location within the Fallopian tube, the velocities will vary accordingly. The greatest concentration of cilia is located in the ampulla, where embryo transport is known to be rapid. While CBF contributes greatly to the fluid mechanical properties of the embryo microenvironment, muscular contractions also have a prominent role as discussed previously. This mechanical force appears to be influenced by chemical cues as well; Wanggren et. al.[20] discovered that during the follicular phase the frequency of muscle contractions was on the order of 3.7/min in human subjects, compared to 4.5/min at the periovulatory phase and 3.2/min at the luteal phase. Furthermore, muscular contraction frequency increased upon treatment with PGF2a and PGE2, and diminished upon treatment with PGE1, progesterone, levonorgestrel, mifespristone, oxytocin, and hCG. Despite the paucity of data regarding muscular contraction in humans and CBF at physiological temperatures, the available information has helped to develop useful computer models for comprehending the influence of mechanical cues on embryo development and transport.

Microfluidic technology to fill the gap between *in vivo* and *in vitro* Fertilization

The widespread use of assisted reproductive technologies, particularly IVF, has compelled scientists and clinicians to take a critical look at the individual steps that compose these procedures. Analysis of these methodologies has led to a greater understanding of reproductive physiology and has improved results. For instance, fertilization rates and

embryo development have improved with enhancements in methods for processing and isolating sperm, effectively augmenting recovery of motile sperm and reducing sperm damage[21]. An emerging technology showing great promise for application in IVF is microfluidics. This technology has been applied extensively in chemistry[22] and molecular biology[23] because it takes advantage of fluid dynamic properties on the micron scale for easy manipulation of microenvironments and handling of small quantities of samples. As early as the 1970s, Walladsen and colleagues reported the importance of microenvironment and embryo handling and culture, through the use of microfluidics[24]. Microfluidic technology can potentially provide controllable microenvironments specialized for embryo development and even provide an automated platform for performing multiple steps of IVF. Subsequent chapters will discuss these applications and advances in this technology.

An important step for ensuring proper embryo development is through selection of high quality oocytes and sperm. In a clinical setting, quality oocyte selection can be very subjective since it involves visual inspection of a population. To this end, Choi et. al.[25] developed a microfluidic device capable of selecting normal oocytes with relatively high specificity; this was achieved by flowing a population of oocytes through a microfluidic channel flanked by electrodes where an alternating current was applied. It was found that normal oocytes demonstrated greater mobility towards the electrodes compared to abnormal oocytes. Similarly, intrinsic mobility was used to distinguish normal sperm from unhealthy sperm in a simple microfluidic platform[26]; using coupled laminar flow streams, sperm with higher motility were able to move from one stream to the other leading to a different collection site, thereby separating motile, healthy sperm from nonmotile, unhealthy sperm. Precise handling of oocytes/zygotes was also demonstrated through a microfluidic tool that

was able to remove the cumulus, necessary for in-vitro production[27]. The same group developed a microfluidic platform for precise control of embryo positioning, movement, and plug formation using pressure driven flow, while showing the ability to remove the zona pellucida for chimera and transgenic production[27]. While these devices provide convenient handling properties for oocytes and embryos, the ultimate goal is to enhance embryo development with this technology. Along these lines, Raty *et. al*.[28] tested static culture of mouse embryos in microchannels and revealed enhanced development in these milieus compared to standard microdrop embryo development; as well, the number of degenerated embryos was reduced in the microchannels. This work demonstrated that the microchannels under static conditions provided an appropriate microenvironment for embryo stage progression, highlighting that the constrained development area improved results perhaps because of enhancements in paracrine and/or autocrine signaling. When a similar setup was used under dynamic conditions, mouse embryo development was reduced compared to static microdrops, providing more credence to the idea that chemical factors are important[29]. However, as discussed by this paper, the fluid mechanical environment cannot be discounted in its role for embryo development. There is a scarcity of data testing the effects of embryo stage progression under flow conditions that more closely mimic the microenvironment of the oviduct. Microfluidic technology represents an optimal method for deciphering the role that mechanical and chemical cues play on embryo development.

Thesis overview

Of the multiple steps of conception, this thesis will focus specifically on embryo culture and selection. Conventional approaches to enhance in vitro embryo development have relied heavily on modifying media formulations and gas environments. The physiological environment of fertilization, however, is much more complex than a bag with chemicals. The environment is dynamic chemically and mechanically. Few options are available to recapitulate such dynamic microenvironments in current assisted reproduction procedures. Realizing such limitations, there have been researches to enhance the culture hardware using microfluidic devices. Subsequent chapters in this thesis will describe: 1. Characterization and Resolution of Evaporation-Mediated Osmolality Shifts that Constrain Microfluidic Cell Culture in Poly(dimethylsiloxane) Devices. 2. A dynamic microfunnel embryo culture system would enhance outcomes by better mimicking the fluid mechanical stimulation and chemical agitation embryos experience *in vivo* from ciliary currents and oviductal contractions. 3. A new computerized microfluidic real time embryo culture and assay device that can perform automated periodic analyses of embryo metabolism over 18 hrs.

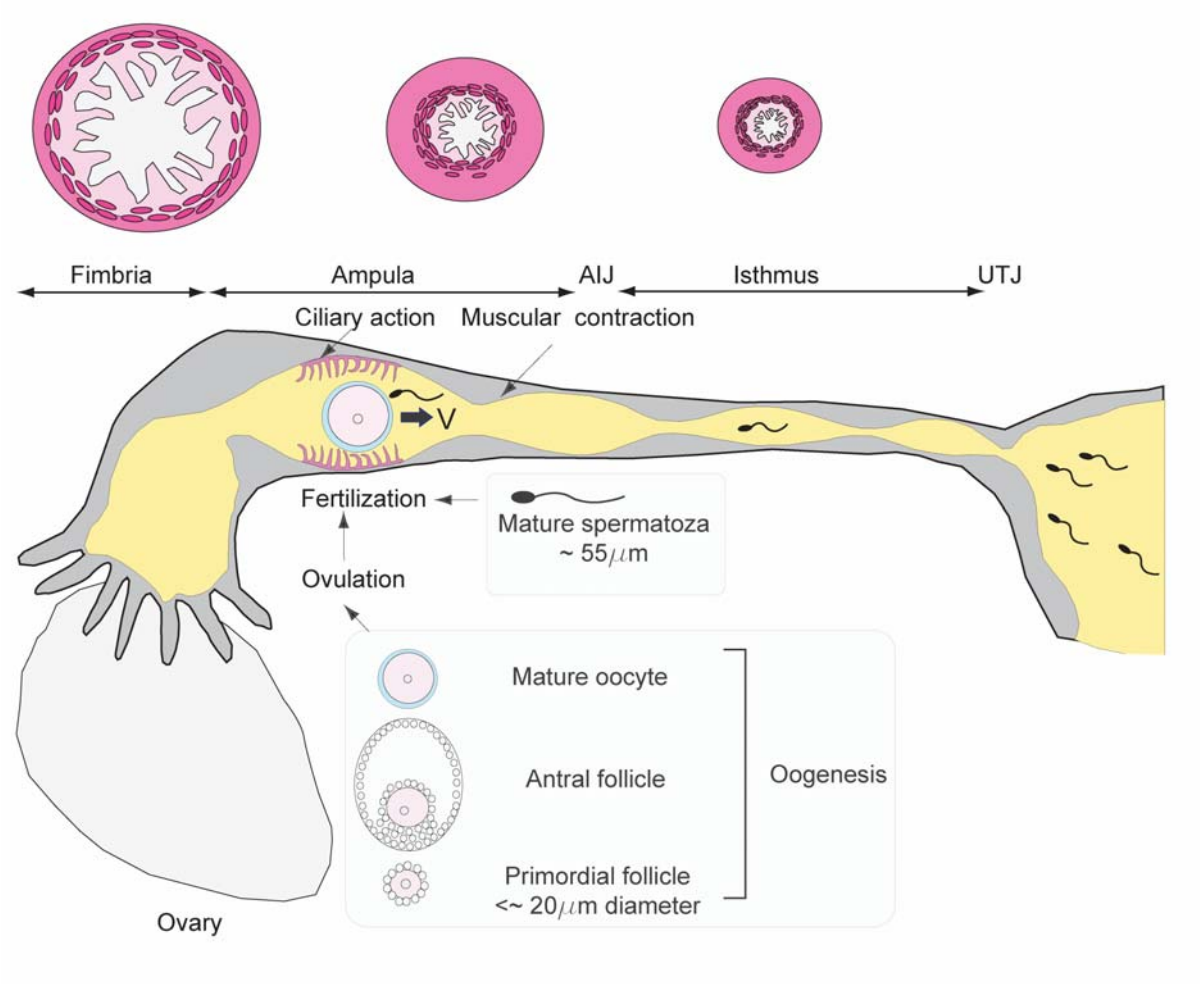

Figure I.1. Sperm migration, oogenesis and microenvironment in human reproduction.

References

[1] Fauci, L. J. & Dillon, R. Biofluidmechanics of reproduction, *Annual Review of Fluid Mechanics* **38**, 371 (2006).

[2] Adashi, E. Y., Rock, J. A. & Rosenwaks, Z., *Reproductive endocrinology, surgery, and technology* (Lippincott-Raven, Philadelphia, 1996).

[3] Clermont, Y. Kinetics of Spermatogenesis in Mammals - Seminiferous Epithelium Cycle and Spermatogonial Renewal, *Physiol. Rev.* **52** (1), 198 (1972).

[4] Gergely, A. *et al.* Morphometric assessment of mature and diminished-maturity human spermatozoa: sperm regions that reflect differences in maturity, *Hum. Reprod.* **14** (8), 2007 (1999).

[5] Barros, C., Vigil, P., Herrera, E., Arguello, B. & Walker, R. Selection of morphologically abnormal sperm by human cervical mucus, *Arch. Androl.* **12 Suppl**, 95 (1984).

[6] Mortimer, D., Leslie, E. E., Kelly, R. W. & Templeton, A. A. Morphological Selection of Human-Spermatozoa Invivo and Invitro, *J. Reprod. Fertil.* **64** (2), 391 (1982).

[7] Ishijima, S., Oshio, S. & Mohri, H. Flagellar Movement of Human-Spermatozoa, *Gamete Res.* **13** (3), 185 (1986).

[8] Drobnis, E. Z. & Overstreet, J. W., in *Oxf. Rev. Reprod. Biol.* (1992), pp. 1.

[9] Scott, M. A. A glimpse at sperm function in vivo: sperm transport and epithelial interaction in the female reproductive tract, *Anim. Reprod. Sci.* **60**, 337 (2000).

[10] Kunz, G. *et al.*, in *Fate of the Male Germ Cell* (1997), Vol. 424, pp. 267.

[11] Neill, J. D. ed., *Knobil and Neill's physiology of reproduction* 3ed. (Elsevier, 2006).

[12] Halbert, S. A., Tam, P. Y. & Blandau, R. J. Egg Transport in Rabbit Oviduct - Roles of Cilia and Muscle, *Science* **191** (4231), 1052 (1976).

[13] Gaddumrosse, P. & Blandau, R. J. Comparative Observations on Ciliary Currents in Mammalian Oviducts, *Biology of Reproduction* **14** (5), 605 (1976).

[14] Lyons, R. A., Saridogan, E. & Djahanbakhch, O. The reproductive significance of human Fallopian tube cilia, *Human Reproduction Update* **12** (4), 363 (2006).

[15] Bourdage, R. J. & Halbert, S. A. Invivo Recording of Oviductal Contractions in Rabbits During the Periovulatory Period, *American Journal of Physiology* **239** (3), R332 (1980).

[16] Blake, J. R., Vann, P. G. & Winet, H. A Model of Ovum Transport, *Journal of Theoretical Biology* **102** (1), 145 (1983).

[17] Holloway, G. A., Halbert, S. A. & Lee, W. I. Fibre-Optic Laser Instrument for Measuring Ciliary Activity of Oviducts Invitro, *Med. Biol. Eng. Comput.* **26** (6), 655 (1988).

[18] Lyons, R. A., Saridogan, E. & Djahanbakhch, O. The effect of ovarian follicular fluid and peritoneal fluid on Fallopian tube ciliary beat frequency, *Hum. Reprod.* **21** (1), 52 (2006).

[19] Mahmood, T., Saridogan, E., Smutna, S., Habib, A. M. & Djahanbakhch, O. The effect of ovarian steroids on epithelial ciliary beat frequency in the human Fallopian tube, *Hum. Reprod.* **13** (11), 2991 (1998).

[20] Wånggren K, Stavreus-Evers A, Olsson C, Andersson E & K., G.-D. Regulation of muscular contractions in the human Fallopian tube through prostaglandins and progestagens, *Hum Reprod* **Jul 11. [Epub ahead of print]** (2008).

[21] Mortimer, D., *Practical Laboratory Andrology*. (Oxford University Press, New York, 1994).

[22] Tomlinson, A. J., Guzman, N. A. & Naylor, S. Enhancement of concentration limits of detection in CE and GEMS: A review of on-line sample extraction, cleanup, analyte preconcentration, and microreactor technology, *J. Capillary Electrophor.* **2** (6), 247 (1995).

[23] Beebe, D. J., Mensing, G. A. & Walker, G. M. Physics and applications of microfluidics in biology, *Annual Review of Biomedical Engineering* **4**, 261 (2002).

[24] Willadsen, S. M. Method for Culture of Micro-Manipulated Sheep Embryos and Its Use to Produced Monozygotic Twins, *Nature* **277** (5694), 298 (1979).

[25] Choi, W. *et al.* Dielectrophoretic oocyte selection chip for in vitro fertilization, *Biomed. Microdevices* **10** (3), 337 (2008).

[26] Cho, B. S. *et al.* Passively driven integrated microfluidic system for separation of motile sperm, *Analytical Chemistry* **75** (7), 1671 (2003).

[27] Zeringue, H. C., Rutledge, J. J. & Beebe, D. J. Early mammalian embryo development depends on cumulus removal technique, *Lab Chip* **5** (1), 86 (2005).

[28] Raty, S. *et al.* Embryonic development in the mouse is enhanced via microchannel culture, *Lab Chip* **4** (3), 186 (2004).

[29] Hickman, D. L., Beebe, D. J., Rodriguez-Zas, S. L. & Wheeler, M. B. Comparison of static and dynamic medium environments for culturing of pre-implantation mouse embryos, *Comparative Medicine* **52** (2), 122 (2002).

CHAPTER II

Characterization and Resolution of Evaporation-Mediated Osmolality Shifts that Constrain Microfluidic Cell Culture in Poly(dimethylsiloxane) Devices

Evaporation is a critical problem when handling sub-microliter volumes of fluids. This paper characterizes this problem as it applies to microfluidic cell culture in poly(dimethylsiloxane) (PDMS) devices and provides a practical solution. Evaporation-mediated osmolality shifts through PDMS membranes with varying thicknesses (10, 1, 0.2 or 0.1 mm) were measured over 96 hours. Even in humidified cell culture incubators, evaporation through PDMS and associated shifts in the osmolality of culture media was significant and prevented mouse embryo and human endothelial cell growth and development. A simple diffusion model, where the measured diffusion coefficient for PDMS matches reported values of $\sim 10^{-9}$ m^2/s, accounts for these evaporation and osmolality shifts. To overcome this problem a PDMS-parylene-PDMS hybrid membrane was developed that greatly suppresses evaporation and osmolality shifts, yet possesses thinness and the flexibility necessary to interface with deformation-based microfluidic actuation systems, maintains the clarity for optical microscopy, and enables the successful development of single cell mouse embryos into blastocysts under static conditions and culture of human endothelial cells under dynamic recirculation of sub-microliter volumes of media. These insights and methods demonstrated specifically for embryo and endothelial cell studies will be generally useful for understanding and overcoming evaporation-associated effects in microfluidic cell cultures.

Introduction

Microfluidic devices offer the ability to work with nano- to microliter volumes of fluids[1,2] and is useful for reducing reagent consumption, creating physiologic cell culture environments that better match the fluid-to-cell-volume ratios *in vivo*[3,4] as well as performing experiments that take advantage of low Reynolds number phenomenon such as subcellular treatment of cells with multiple laminar streams[5,6]. Many microfluidic systems are made of poly(dimethylsiloxane) (PDMS) because of its favorable mechanical properties, optical transparency, biocompatibility[7,8], and its straightforward manufacturing by rapid prototyping[9]. A common challenge with PDMS based microfluidic chips, however, is evaporation through PDMS. Evaporation is especially detrimental to cell culture in microfluidic chips because even the slightest amount of evaporation from the small liquid volumes present in microfluidic systems results in a significant increase in osmolality. It is well-documented that elevated osmolality can affect ion balance[10], cellular growth rate[11], metabolism[12,13], antibody production rate[14], signaling[15], and gene expression[14,16]. In general, the osmolality of the extracellular environment is normally ~300 mmol/kg. Tolerance to higher osmolalities is cell type dependent. While Chinese Hamster Ovary (CHO) cells and a variety of hardy cell lines tolerate and proliferate under a wide range of osmolality (300-500 mmol/kg)[13], more sensitive cells such as mammalian gametes and embryos will undergo a development that is blocked at osmolalities significantly lower or higher than 265 to 285 (mmol/kg)[17]. Here, we provide a quantitative understanding of the relationship between evaporation and osmolality shift of cell culture media in microfluidic devices constructed of various

thicknesses (0.1 to 10 mm) of PDMS and show how devices with thin PDMS layers lead rapidly to large osmolality shifts that result in cell death. Furthermore, we describe methods to greatly suppress such osmolality shifts using membranes with low water permeability and perform two biological demonstrations: 1. Static microfluidic culture of single cell embryos to blastocysts in submicroliter volumes of fluids over 4 days using a humidified incubator; and 2. Dynamic culture of primary human endothelial cells with recirculation of submicroliter volumes of media over 10 hours without media refreshment in a non-humidified environment.

There are several remedies against evaporation from PDMS devices such as: placement of water-filled reservoirs on-chip[18,19], submerging the whole chip in water[20], application of PCR-tape to the chip[21,22], use of oil to cover aqueous liquids[23,24], and changing of curing agent to base ratio[25]. Although useful and beneficial for many applications, these methods also have drawbacks and limitations such as limiting the environment that the chip can be used in, altering optical access, hindering interfacing to external devices such as Braille display-based microactuator arrays, or simply being messy. In addition, there are no previous reports that quantitatively measure the effects of on-chip evaporation on osmolality, a factor particularly important for cell viability. In this paper, we quantify the rate of evaporation and its effect on composition of cell culture media by measuring the rate of osmolality shifts in PDMS chips with different thickness membranes over a 4 day period inside a humidified cell culture incubator. In spite of the humidified environment (typically 85% humidity) of a cell culture incubator, significant evaporation was measured with thinner PDMS membrane devices having a more dramatic shift in osmolality and a correspondingly worse development rate for

embryos, where a majority of embryos stop development at the two cell stage or in approximately 24 hours. In heated yet non-humidified environments, such as portable handheld cultures with real-time video microscopy[26], in–channel evaporation is even faster leading to cell death in less than an hour in the absence of media refreshment. Although parylene has been coated onto PDMS previously to prevent evaporation during micro PCR[27], there was little consideration for support of cell growth and viability, mechanical stability, or ability to perform optical microscopy. We describe the use of a "hybrid membrane: PDMS-parylene-PDMS" that can prevent evaporation while maintaining a permissive environment for cell growth and also providing necessary flexibility, mechanical durability against cracking, and thin profile that is required to perform deformation-based microfluidic pumping and valving using piezoelectric pin actuator arrays on refreshable Braille displays[28]. The insights and methods described should be broadly useful for advancement of microfluidic cell cultures and assays where prolonged submicroliter cell cultures need to be performed in PDMS devices.

Experimental Section

Glass wells and PDMS membrane preparation. Slide glasses (75x25x1 mm) having 4 holes with a 6.5 mm diameter and placed 1.5 cm apart were used for evaporation and osmolality shift measures as shown in Figure II. 1a. Glass slides were used to avoid contact of oil with PDMS which could potentially lead to unwanted side effects of oil adsorption into the PDMS membrane. Membranes of PDMS with different thickness such as 0.1mm or 0.2mm, 1mm and 10mm were irreversibly bonded to the

slide glass after O_2 plasma treatment. Additional reservoir structures were attached to each hole to hold mineral oil. In each well, 50µl of Potassium Simplex Optimized Medium (KSOM; Specialty Media, Phillipsburg, NJ) + 0.1% Serum Substitute Supplement (SSS; Irvine Scientific, Santa Ana, CA) was loaded and covered with a layer of 500µl of oil as shown in Figure II.b. Conventional microdrop, using 50µl KSOM and covered with oil in a culture dish, was used as control. All prepared devices were placed into a typical humidified cell culture incubator environment (85% humidity) of 5% CO_2 in air at 37°C and equilibrated overnight.

Embryo preparation. Six- to eight-week-old B6C3F1 female mice (Charles River) were superovulated by an intraperitoneal administration of 10 IU of pregnant mare serum gonadotropin (PMSG; Sigma Chemical Co.) by injection, followed 44h later with an injection of 10 IU human chorionic gonadatropin (hCG; Sigma Chemical Co.). Presumptive zygotes were collected 18 h later by dissecting oviducts in Hepes-buffered Human Tubal Fluid medium (HTFH; Irvine Scientific) supplemented with 0.1% (w/v) hyaluronidase to remove surrounding cumulus cells. All procedures performed on animals were approved by the University of Michigan Animal Care and Use Committee. Zygotes were placed into 50µl of KSOM + 0.1% SSS overlaid with mineral oil in either organ culture dishes (control), or glass-wells with PDMS membranes of 10 (PDMS-10), 1.0 (PDMS-1), or 0.1 (PDMS-0.1) mm thick. Zygotes and culture devices were placed into a humidified environment of 5% CO_2 in air at 37°C. Embryos were assessed at 24hr intervals. Nonparametric measures of time-appropriate development to ≥ 2-cells at 24hrs

and ≥ 4-cells at 48hr were compared by chi-square analysis. Differences were considered significant at $P<0.05$.

Osmolality measurement. Wescor's Vapor Pressure Osmometer, VAPRO (Wescor Inc, Utah, USA) was used to measure the osmolality. Each glass-PDMS well was filled with 50µl KSOM and overlaid with oil. Change in osmolality of the KSOM media in the wells was measured at 24hr intervals over a total of 96 hour period. To measure osmolality, 10µl of KSOM was taken from each well and placed on sample loading area in VAPRO. For each run VAPRO was calibrated using Wescor's Optimol® osmolality standards. Statistics were performed using mixed linear regression and differences considered significant at $P<0.05$.

Parylene deposition. For parylene coated PDMS, 2.5 or 5µm thick layer of parylene C was deposited on the backside of PDMS membranes by using a PDS 2010 labcoater (Specialty Coating Systems) after covering the well side with a PDMS membrane.

Device Fabrication for microfluidic culture of embryo. The Microfluidic device (Figure II. 4a) was composed of a thick (~ 8mm) PDMS slab with microfluidic channel features, fabricated by using soft lithography[9], attached to a thin PDMS or PDMS-parylene-PDMS hybrid membrane. The thick PDMS slab with channel features was prepared by casting prepolymer (Sylgard 184, Dow-Corning) at a 1:10 curing agent-to-base ratio against positive relief features. The relief features were composed of SU-8

(MicroChem, Newton, MA) and fabricated on a thin glass wafer (200μm thick) by using backside diffused-light photolithography[29]. The prepolymer was then cured at 60°C for 60 min, and holes were punched in it by a sharpened 14-gauge blunt needle. The PDMS-parylene-PDMS hybrid membrane was prepared by the following stepwise procedure: spin coating PDMS onto a 4″ silanized silicon wafer to a thickness of 100 μm, curing this layer at 120°C for 30 min, depositing a 2.5 or 5 μm thick parylene layer using a PDS 2010 labcoater, plasma oxidizing the resulting parylene surface for 90 seconds, and spin coating another 100 μm thick layer of PDMS and curing to get a total thickness of ~200 μm.

Device Fabrication for Microfluidic Endothelial Cell Culture. The microfluidic device for endothelial cell (EC) culture was fabricated as was described previously.[18] Briefly, three layers of cured poly(dimethylsiloxane) (PDMS) at a ratio of 1:10 base to curing agent were sealed together irreversibly using plasma oxidation (SPI supplies, West Chester, PA). Unless stated otherwise, the PDMS layers were cured overnight at 60°C. The top of the three layers (~1 cm thick) contains a rectangular shaped fluid reservoir (Figure II. 6a). The middle layer (~1 mm thick) consists of bell-shaped channels features[29] ~30 μm in height and 300 μm in width formed using soft lithography[9]. The channel features of the middle layer face downward and are sealed against a thin membrane bottom layer which is the substrate for cell attachment. PDMS-only thin membranes were fabricated by spin coating freshly mixed 1:10 PDMS onto silanized (75 x 50 mm, 1mm thick) glass slides (Corning Glass Works, Corning, NY) to a uniform thickness of either ~120 and 400 μm and then cured overnight at 120°C. For

experiments involving parylene coated membranes, the same PDMS-parylene-PDMS hybrid thin membrane described above with a total uniform thickness of 200 μm was used.

Fluid Actuation System. The computer-controlled Braille display fluid actuation scheme is based on a design described previously[26] with minor modifications to make the system more compatible with inverted phase contrast microscopy[30]. The Braille display used (SC9; KGS, Saitama, Japan) was powered by a universal serial bus (USB) and consisted of 6 actuation cells, each containing 8 piezoelectric Braille pins (6 × 8 = 48 pins).

Indium tin oxide (ITO) Heater. The ITO heater was constructed by an ITO layer deposited on a glass slide with metallic films for electric contact. First, the glass slide was masked using scotch tape to form the pattern for the ITO layer. An ITO with a thickness of ~1500Å was coated on a 75x25x1 mm slide glass using radio frequency sputtering (Enerjet Sputter) as shown in Figure II. 5a. This is followed by removing the masking tapes and annealing the device in a 650^{o}C convection oven for 1 hour. The resulting sheet resistance of the annealed ITO layer is ~30 Ω/square. In order to smoothly generate electric current through the ITO layer for uniform joule heating,two aluminum strips (1 mm width and 2000Å thick) were patterned and coated in a similar manner on two edges of the ITO layer. Electrical wires were attached to the aluminum stripes using silver epoxy glue to form connections to external control circuits. A commercially available wire thermocouple (5TC-TT-J; Newport, Santa Ana, CA) was

attached onto the heater surface for temperature sensing. All the wires were connected to a microprocessor based temperature control unit (CT16A2088, Minco Products, Inc., Minneapolis, MN) for feedback control of the heater surface temperature. As a result, the heater surface can be maintained constantly at desired temperature. The advantages of this ITO heater are: 1. Excellent optical transparency in visible light wavelength range. 2. Less image distortion than thin film heater (Ref. 26). 3. More uniform heating over large areas.

(General) Endothelial Cell Culture. Human dermal microvascular endothelial cells (HDMECs, Cambrex, East Rutherford, NJ) were cultured in endothelial growth media-2 MV (EGM-2 MV, Cambrex) in T-25 culture flasks (Corning, Acton, MA) that were placed in a humidified 5% CO_2 cell culture incubator. The HDMECs were collected by washing and detaching with 0.25% Trypsin/EDTA (Invitrogen, Carlsbad, CA). The Trypsin solution was neutralized with 10% FBS in DMEM and spun down with a centrifuge (ThermoForma, Marietta, OH) for 5 min, 4^{o} C, 800 RPM. The supernatant was removed and the pellet was resuspended in EGM-2 MV. The spin and resuspension in EGM-2 MV was repeated to ensure removal of Trypsin which inhibits cell adhesion during seeding.

Cell Seeding and Microfluidic Cell Culture. To facilitate cell attachment, the channels were coated for 30-60 min at room temperature with 5-10 μl of human plasma fibronectin (FN) solution (Invitrogen) at a concentration of 100 g/ml PBS shortly after plasma oxidation (5-10 min). The FN solution was introduced through holes punched

with a dermal biopsy puncher (Miltex Inc., York, PA)) though the top and middle layer prior to sealing with plasma oxidation to act as seeding ports by being compatible for use with micropipette tips. After cell seeding (described below), the seeding ports were covered with a sterilized glass slide to avoid contamination when present in non-sterile conditions. After coating, the FN solution was rinsed for 10 minutes with PBS that was pumped through the channels from the fluid reservoir. Afterwards, the device was sterilized by placing under UV light for ~30 minutes. Following UV sterilization, PBS was replaced with endothelial growth media-2 MV (EGM-2 MV, Cambrex, East Rutherford, NJ) which is supplemented as a kit prior to use with 5% fetal bovine serum (FBS) and a host of growth factors/supplements such as vascular endothelial growth factor (VEGF). EGM-2 MV was circulated overnight for the serum proteins to coat the PDMS surface along with FN to facilitate cell attachment. All reagents were added under sterile conditions.

A small amount (3-5 μl) of a dense (~10^7 cells/ml) HDMEC suspension was pipeted into the cell seeding port and introduced into fluidic regions defined by the Braille pins acting as valves via gentle application of positive pressure. After the HDMECs were seeded, all channels were valved to trap the cells and the PDMS chip and the Braille display were placed in a 37^{o}C/5% CO_2 incubator to allow for the cells to attach for 60-90 minutes. After the cells attach, EGM-2 MV culture media was circulated from the fluid reservoir (Supplementary info) for the next 24-72 h until the cells reach confluence.

Recirculating Fluid Actuation. Experiments conducted with recirculation of small amounts of fluid (~500 nl) were conducted on the stage of an inverted microscope (Nikon TS-100F, Japan), imaged with a 10x Ph1 objective (Achromat), and recorded using Coolsnap CF2 Camera with MetaVue software. To account for the lack of controlled temperature and 5% CO_2 tension provided by a cell culture incubator, the bottom of the PDMS device was heated to 37^{o}C (ITO heater, PID Temperature Controller, Minco, Minneapolis, MN) and the culture media was specially formulated with a synthetic buffer to maintain stable pH of ~7.3 under ambient conditions[26]. Braille pins were reconfigured via computer-control such that flow can only occur in the recirculation loop (Figure II. 6a) due to complete valving. The initial amount of fluid continuously recirculated was ~500 nl at a pumping frequency of 0.125 Hz. Images were recorded at the intersection of the "X" towards the center of the microfluidic device (Figure II. 6a). The cell density was recorded for discrete time points and normalized to the value at T=0. Cells were considered still alive if they remained attached and were still moving (visualized with real-time microscopy). For PDMS-only membranes, two experiments were performed in duplicates; for the Parylene membrane device, only one experiment was performed.

Results and Discussion

Osmolality measurement and diffusion coefficient. As described above, glass slides were drilled to form 6.5 mm diameter holes and the slide sealed against PDMS membranes with thicknesses of 0.1, 0.2, 1.0 and 10 mm to form wells. Fifty μl of KSOM

was added to the wells, overlaid with oil, and the osmolality of the media assessed at 24hr intervals. As shown in Figure II. 2a, the osmolality increased significantly over a 96 hour period, with greater shifts observed as the membrane became thinner. The increase in osmolality was particularly significant for thin PDMS membranes of 0.1 and 0.2 mm that are commonly used for pin-actuator based fluid actuation systems.

Closer analysis of the data provides useful quantitative insights into the characteristics of PDMS as well as how careful one needs to be when handling small amount of media. Silicon elastomer membranes are known for their selective permeation properties with gases and liquids. The diffusion of water through silicone has been measured experimentally[31,32], and interpreted theoretically[33]. These reports suggest that the classical Fick's model of diffusion, although not perfect, describes diffusion of water through PDMS reasonably well. In our experiments, we calculate the flux of water, and the diffusion coefficient of water through PDMS using measured osmolality values and Fick's laws of diffusion.

Osmolality is defined as a measure of the number of dissolved particles (ions and undissociated molecules, such as glucose or proteins) per kg of water[34]. O^* represents the total number of dissolved particles, assuming constant over the time, O is the measured osmolality (mmol/kg), m is the total mass (kg) of the media. The change in mass and change in osmolality is inversely proportional. Thus,

$$O(mmol/kg) \times m(kg) = O^*, \; m(kg) = \frac{O^*}{O} \qquad \textbf{(1)}$$

$$\therefore \frac{m_2}{m_1} = \frac{\frac{O^*}{O_2}}{\frac{O^*}{O_1}} = \frac{O_1}{O_2} \qquad \textbf{(2)}$$

When J is defined as the mass flux through a unit area per unit time [kg/m^2·s]. Δm is mass change with given time. A is area [m^2], which is area of 6.5 mm well in this case. t is time [s], which is 24hour in this case.

$$J = -\frac{\Delta m}{A \cdot t} = \frac{1}{A \cdot t} \cdot (m_1 - m_2) = \frac{1}{A \cdot t} \cdot \left(m_1 - \frac{O_1}{O_2} \cdot m_1 \right) = \frac{m_1}{A \cdot t} \cdot \left(1 - \frac{O_1}{O_2} \right) \quad \textbf{(3)}$$

By Fick's 1st law, J can be also described as:

$$J = -D \cdot \frac{dC}{dx} = D \cdot S \cdot \frac{(P_s - P)}{dx} = D \cdot S \cdot P_s \cdot (1 - P/P_s) \cdot \frac{1}{dx} \approx k \cdot \frac{1}{x} \propto \frac{1}{x} \quad \textbf{(4)}$$

Equation 3 provides a plot of J with respect to 1/x as shown in Figure II. 2b where the slopes, k, are between $10^{-10} \sim 2 \cdot 10^{-10}$[kg/m·s]. Based on equation 3 and Fick's 1st law (eq 4) we find that these slopes give diffusion coefficients, D, of $3 \times 10^{-9} \sim 6 \times 10^{-9}$ [m^2/s], which is consistent with previously reported value[31-33]. Here, the humidity at the media surface is considered to be 1 (100% humidity), the humidity of our incubator was measured to be approximately .85 (85% humidity), the saturated vapor pressure (P_s) at 37°C is 6.33×10^3 Pa, P is the vapor pressure outside of the chip's environment, P/P_s is 0.85, the water solubility coefficient (S) in PDMS is approximately 1.04 [$(cm^3)_{water}$/cmHg·$(cm^3)_{PDMS}$][35] and the saturated vapor specific volume (V_g) at 37°C is $V_g \approx 22.94(m^3/kg)$, $\rho_g = 0.0436(kg/m^3)$[36].

An observation not explained by evaporation of water through PDMS is the osmolility shift from 265 to 280 (mmol/kg) over the first 24 hours, even in control experiments that did not use PDMS. Absorption of water by the oil used to cover the media only account for a very small portion (2% or 0.0540mg) of the lost water[37]. Thus,

the majority of the loss is due to evaporation occurring during the few minutes of handling between transfer of droplets from a macroscopic bottle of media to a well and covering it with oil. This underscores not only the importance of preventing evaporation from media in the chip, but also how crucial it is to prevent evaporation during transfer of fluids onto the chip.

Embryo culture and Osmolality. As described above for measurement of osmolality shifts, the collected zygotes were placed into 50µl of KSOM + 0.1% SSS overlaid with mineral oil in either organ culture dishes (control), or in cover-glass wells with PDMS floors of 10 (PDMS-10), 1.0 (PDMS-1), or 0.1 (PDMS-0.1) mm thickness. As shown in Figure II. 3a, there was no significant difference in the ability of zygotes to develop to/beyond the 2-cell stage at 24hrs of culture in control (73%), PDMS-10 (81%), PDMS-1 (88%), or PDMS-0.1 (80%). However, at 48hrs, significantly fewer zygotes ($P<0.01$) had developed to/beyond the 4-cell stage in PDMS-0.1 (22%) compared to control (67%), PDMS-10 (67%) and PDMS-1 (72%). The compromised development of embryos in PDMS-0.1 (Figure II. 3a), where the measured osmolality at 24-48 hrs is well above 300 mmol/kg (Figure II. 2a), is consistent with the known tendency of embryo development to be arrested at high osmolalities[17]. Thus, one cannot perform embryo culture in microfluidic devices with thin membranes composed solely of PDMS or the type of membrane commonly used for deformation-based microfluidic actuation systems. Although embryos have been previously cultured in PDMS/borosilicate hybrid microfluidic devices under static conditions[38], little consideration was given to the evaporation through PDMS due to its thickness. In both the previous system and our

current system, most of the evaporation occurs through the bottom PDMS layer but the amount of evaporation in our system is much greater because the PDMS membrane is much thinner. We also investigated the effect of pre-soaking PDMS in culture media or mineral oil for 24 hours, but saw little or no improvement (data not shown).

Next, we coated 2.5 um parylene on the outer side of a 0.1mm-PDMS membrane or simply applied plastic tape. Parylene is deposited by a unique vapor deposition polymerization process, and the resulting coatings are pinhole free and can easily conform to surface shapes while maintaining a uniform thickness. Both parylene coated PDMS and tape made evaporation through the membrane negligible, as shown in Figure II. 3b. (The slight shift from 265±5.1 to 285±1.2 mmol/kg is attributed to evaporation during transfer of fluid not evaporation through the membrane.) Importantly, the parylene coating significantly improved blastocyst development (87±14 blastocyst development) compared to the identical system with no parylene (2±4; $P<0.01$; Figure II. 3c). Tape was not tested for embryo development, however, because it is thick and unfavorable for deformation-based microfluidic actuation systems and the adhesive on the tape may be toxic to cells.

To perform microfluidic embryo culture, we fabricated a two-level fluidic system using a two-step photolithography procedure. First, a 30μm high bell-shaped channel for Braille actuation was formed by backside diffused-light photolithography[29] then a 200μm high rectangular channel for introducing embryos was aligned and formed by conventional photolithography. Next the PDMS-Parylene-PDMS "hybrid" membrane with a bottom well (80μm depth) for trapping[39] was used to seal the channels. Embryos were introduced into the "Snake head-like" culture chamber with a well, as shown in

Figure II. 4b using fluid pumping action generated by manual deformation and release of the culture media reservoir with fingers. As shown in Figure II. 4c, one cell embryos were successfully cultured into blastocysts using the PDMS micro device with the "hybrid" membrane, under static conditions, without changing the culture medium over the 96 hour culture period. When one cell embryos were cultured using a PDMS micro device with the same thickness, but without the "hybrid membrane", the cells did not develop into blastocysts. The insights and methods described should be broadly useful for advancement of microfluidic cell cultures and assays in general and for increasing application, acceptance, and subsequent efficiencies in mammalian gamete/embryo culture and success of assisted reproductive technologies in biomedical research (transgenic mice), genetic gain and domestic animal production, and treating human infertility.

Use of Parylene Coated PDMS Membranes in Deformation-Based Fluid Actuation. We further tested the applicability of the parylene coated PDMS devices to actively actuated Braille microfluidic systems and to other cell types. When parylene was simply coated on the outside and the PDMS microfluidic chips which are subjected to repeated deformation-based fluid actuation using piezoelectric pin actuators of a refreshable Braille display, the parylene membrane became scratched, scarred, and cracked. To address this problem of cracking, a "hybrid" membrane was developed that sandwiched parylene between two layers of thin PDMS as seen in Figure II. 5. First, a 100μm PDMS membrane (Figure II. 5a I) was formed on a silanized 4″ silicon wafer followed by deposition of a 2.5μm film of parylene (surface II). The resulting parylene

surface was plasma oxidized and covered with a spin-coated layer of PDMS (100μm) to form surface III. This "hybrid" membrane (surface I, II, III) was irreversibly bonded to a PDMS mold containing channel features to form the microfluidic chip. As shown in Figure II. 5b and c, the channels are fully compatible with deformation-based fluid actuation using pin actuators.

Endothelial Cell Survival Under Recirculating Fluid Actuation. Using the deformation-based fluid actuation described above that incorporates a PDMS-parylene-PDMS hybrid membrane, we also tested sub-microliter recirculating culture of human dermal microvascular endothelial cells (HDMEC) in a non-humidified environment with on device heating. This type of capability is expected to be important for future studies of the effect of autocrine and paracrine effects on endothelial cells under fluid perfusion conditions.

Confluent monolayers of HDMECs were seeded and cultured within the microfluidic device and imaged at the intersection of the "X" region (Figure II. 6a). Figure II. 6b is a timelapse comparison of HDMEC survival under continuous recirculation of ~500 nl of media with deformation-based Braille fluid actuation. The experimental conditions were 120 μm thick, PDMS-only membrane ("thin PDMS"); 400 μm thick, PDMS-only membrane ("thick PDMS"); and 200 μm thick, PDMS-parylene hybrid membrane ("hybrid"). At T = 40 (time given in min), virtually all the cells in the visualized region for the "thin PDMS" membrane are dead and detached whereas the cells for the "thick PDMS" and "hybrid" membranes remain confluent. At T = 80,

virtually all the cells for the “thin PDMS” and “thick PDMS” membranes are dead and detached whereas the “hybrid membrane” still remains confluent.

The results were quantified by counting the changes in cell density with time due to continuous recirculation (Figure II. 6c). For the “thin PDMS” membrane, about 50 percent of the cells were dead and detached by about T = 25 (extrapolating from data in Figure II. 6c) and all of the cells were gone by T=50. For the “thick PDMS” membrane, about 50 percent of the cells were dead and detached by T = 65 and all of the cells were gone by T = 90. With the “hybrid” membrane, cells survive much longer under continuous recirculation than the PDMS-only membranes. Cells remain roughly confluent (>85 percent of the original cell density) up to T = 720 (or 12h). Afterwards, cells begin to die more rapidly with 50 percent of the cells remaining alive and attached at about T=800 (13.3h) and less than 5 percent at T = 1080 (18h) (Figure II. 6c). By comparing the times it takes for 50 percent of the cells to die, we conclude that cells are able to survive about 2.6 times longer with the “thick PDMS” membrane compared to the “thin PDMS” membrane. In addition, cells are able to survive about 29 times as long with the “hybrid” membrane when compared with the “thin PDMS” membrane and 11 times as long when compared with the “thick PDMS” membrane. Thus, the integration of parylene in the “hybrid” membrane substantially increases the time HDMECs survive under continuous recirculation of ~500 nl of fluid even though at 200 μm, the “hybrid” membrane is slightly thicker than the “thin PDMS” membrane (120 μm) and half as thick as the “thick PDMS” membrane (400 μm).

Further analysis of evaporation rates, using the simple diffusion equation suggested above, is useful in understanding the different cell survival ratios under

continuous recirculation with diverse membranes. Simply comparing 100μm-PDMS with 8mm-PDMS, the flux J through the 8mm-PDMS is approximately 1.25 % of the flux through the 100μm-PDMS. So the majority of evaporation on the PDMS chip with a thin membrane occurs from the bottom thin PDMS membrane. In addition, the amount of evaporated water escaping through the thicker, top PDMS (~8 mm thickness) can be compared with the amount of water evaporated through the thin bottom parylene (~2.5 μm thickness) using the simple diffusion equation:

$\frac{J_{parylene}}{J_{PDMS}} = \left(\frac{D_{parylene}}{D_{PDMS}}\right) \cdot \left(\frac{S_{parylene}}{S_{PDMS}}\right) \cdot \left(\frac{x_{PDMS}}{x_{parylene}}\right)$. The diffusion coefficient of Parylene C for water at 30°C is 2.60 $x10^{-13}(m^2/s)$,[40] which is 4 orders lower than that of PDMS. The thickness of 2.5μm-parylene is 3200 times smaller than that of 8mm-PDMS. The solubility coefficient of Parylene C for water at 40°C is 0.62 $[(cm^3)_{water}/cmHg \cdot (cm^3)_{Parylene}]$[40], which is 0.6 times smaller than that of PDMS. Finally, the flux J through the thin 2.5-parylene is only 24.8% of the flux through the much thicker top PDMS (~8mm). This does suggest that evaporation through the thicker top PDMS as well as partly the bottom 2.5-parylene membrane will be an eventual cause of osmolality shifts even on the "hybrid" membrane chips if the experiment goes on for a long period. In most experiments, partial refreshment of the sub-microliter culture media from a larger on-chip reservoir at least every several hours is envisioned and the current system would function just fine. When longer experiments (days and weeks) are desired in non-humidified environments without refreshing the sub-microliter volumes of media, then additional considerations would be needed, such as moisture barriers for the top side of the chip and increasing the bottom parylene thickness, to further reduce loss of water.

Analysis of osmolality shifts using the simple diffusion equation also gives us a better explanation of why the HDMECs died within 25 min with a 120μm–PDMS bottom membrane. Combining equation (3) and (4), $\frac{\Delta m}{A \cdot t} = D \cdot S \cdot P_s \cdot (1 - P/P_s) \cdot \frac{1}{dx}$ (5). Based on the channel design in Figure II. 6a, approximate values of variables are: channel area, A = 1.473×10^{-5} m^2, $\Delta m = 2.21 \times 10^{-7}$kg [1000 kg/$m^3$ x 0.5x channel volume (4.42×10^{-10} m^3)], D = (3~6)$\times 10^{-9}$ m^2/s, S = 1.04 [$(cm^3)_{water}$/cmHg·$(cm^3)_{PDMS}$][35], P_s at 37°C = 6.33×10^3, $P/P_s = 0.25$, dx = 120×10^{-6} (m). Assuming the initial osmolality of media for HDMECs as ~260 mmol/kg, the osmolality inside the microfluidic channels after 30~60 minutes is expected to be at least 520 mmol/kg and explains why the majority of HDMECs died. Here, the humidity at the media surface is considered to be 100% humidity at 37°C, the humidity of the room was measured to be approximately 25% humidity at 20°C, and the saturated vapor specific volume (V_g) at 37°C is $V_g \approx 22.94(m^3/kg)$, $\rho_g = 0.0436(kg/m^3)$[36].

In addition to osmolality, the oxygen in the media present in chips is most likely the limiting nutrient source and its depletion may affect cell survival over time. Oxygen is an important substrate for cell growth and severe depletion would affect cell growth. However, thinner membranes have faster oxygen permeation and less depletion. Therefore, we do not believe that the difference in cell survival described is due to oxygen depletion. This conclusion is supported further by Ref. (30) which details oxygen measurement and consumption in microfluidic PDMS cell culture devices.

Conclusion

Compared to conventional cell cultures performed in Petri dishes with low cell volume to extracellular fluid volume (CV/EV) ratios, microfluidic environments with large CV/EV ratios have many advantages in terms of cellular self-conditioning of their surrounding medium[4]. Systems with large CV/EV ratios, however, typically also possess large surface to volume (SAV) ratios which increases the rate of evaporation and presents a challenge, particularly when using microfluidic devices made of water vapor permeable materials such as PDMS. Although understanding and preventing evaporation is important for microfluidic applications generally, it is particularly crucial for sensitive mammalian cell culture applications where even relatively small shifts in osmolality can drastically alter cell behavior. Our study provides five main conclusions: i) Osmolality shifts of media in PDMS devices are well approximated by simple diffusive flux models of water vapor through PDMS. Thus, evaporation-mediated osmolality shifts are particularly rapid when using devices with thin PDMS components; ii) Preimplantation mouse embryos are highly sensitive cells and their development is affected greatly by osmolality shifts such as will occur in devices with thin PDMS membranes even in typical humidified cell culture incubators; iii) Under non-humidified conditions with heating, both the 120μm- and 400μm–PDMS bottom membranes limit HDMEC survival to 25-65 minutes. iv) PDMS-parylene-PDMS "hybrid" membranes can prevent such evaporation while also providing the mechanical flexibility needed to be compatible with deformation-based microfluidic actuation systems and the optical clarity needed for cell imaging; and v) Microfluidic systems that incorporate the thin hybrid membrane can successfully develop single cell embryos to the blastocyst stage and culture human endothelial cells for prolonged periods under a non-humidified environment, whereas

devices that use PDMS-only membranes cannot. The better quantitative understanding of how the osmolality of cell culture media changes in PDMS devices may be useful in accounting for and remedying such shifts in culture or for application where changes in the osmolality of media in a controlled manner during culture is necessary[41]. The ability to stabilize evaporation in PDMS chips compatible with pin actuator-based computer controlled pumps and valves using the PDMS-parylene-PDMS hybrid membrane expands the ability to perform convenient and versatile microfluidic cell and embryo culture experiments where fluid circulation and exchange can be regulated to mimic the dynamic culture environments *in vivo* or to manipulate reagents for long-term on-chip assays as well as to better control passive pumping using permeation-driven flow[42,43].

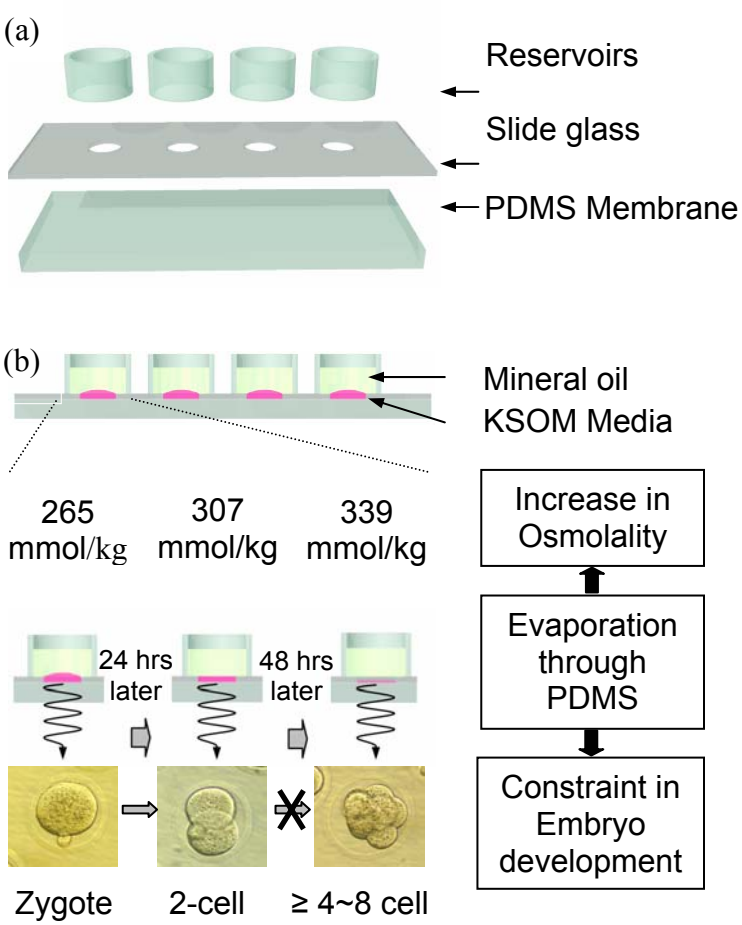

Figure II.1. Experimental set up for osmolality measurements. (a) Schematic design of slide glass with 6.5 mm diameter holes attached to PDMS membranes of 10, 1.0 or 0.1mm thickness to form wells. (b) A cross-section showing the glass-PDMS hybrid structure filled media and overlayed with mineral oil. Evaporation through PDMS increases osmolality in media and constrain embryo development. The displayed values are the measured average osmolality in PDMS-0.1 at 24hours intervals. At 48 hours the osmolality shifts from 265 mmol/kg to 339mmol/kg, and embryos development is blocked accordingly at the 4~8 cell stage. (c) A photograph of an actual device filled with media and mineral oil.

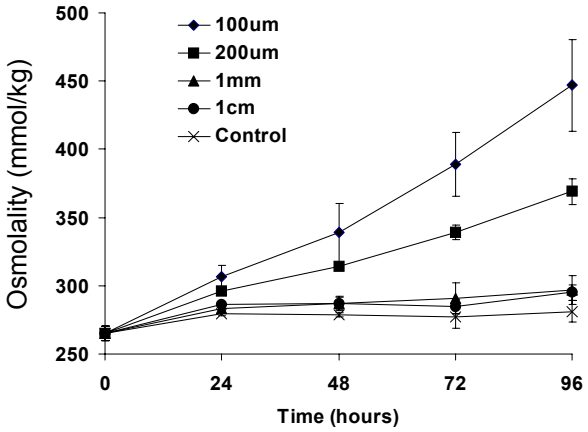

(b)

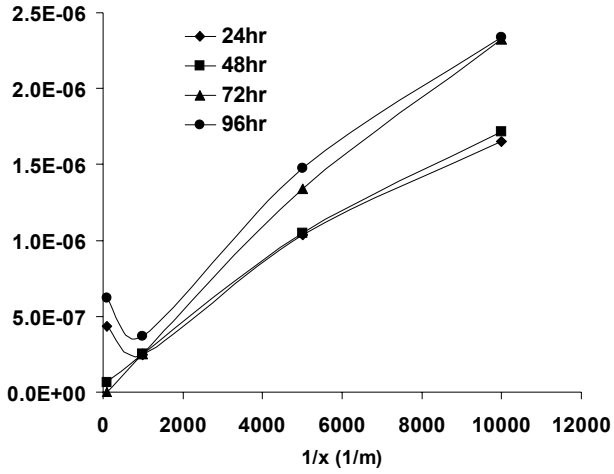

Figure II.2. Osmolality measurements with PDMS membrane. (a) Osmolality of media (KSOM + SSS) over time when cultured in control (organ culture dish) and glass-slide wells with PDMS membrane bottoms of varying thickness. Osmolality changes over time were significantly different for PDMS 0.1mm compared to remaining treatment groups $P<0.01$. (b) Based on equation 3, Flux J was plotted with respect to 1/x using the measured osmolalities with varying PDMS thicknesses.

Figure II.3. Embryo development with different types of membranes. (a) Mouse pronuclei (PN) zygote development in control (organ culture dish) and glass-slide wells with different thickness PDMS membranes. (b) Parylene was coated on the mounted PDMS outside surface with 2.5um thickness and then osmolality change was measured. Osmolality of KSOM drifted from 265 to 285 mmol/kg during 96hrs of incubation in parylene coated PDMS-0.1. (c) Percent blastocyst development was significantly improved with parylene coating (87±14 blastocyst development) compared to no parylene (2±4; $P<0.01$). (d) blastocyst images taken from parylene coated PDMS-0.1 well.

(a)

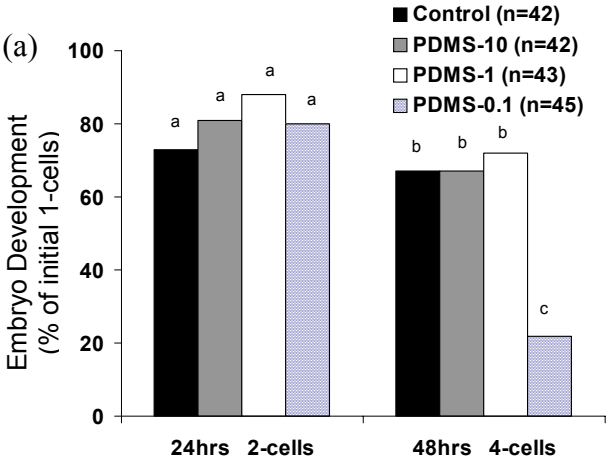
Control (n=42)
PDMS-10 (n=42)
PDMS-1 (n=43)
PDMS-0.1 (n=45)
Embryo Development (% of initial 1-cells)
100
80
60
40
20
0
a
a
a
a
b
b
b
c
24hrs 2-cells
48hrs 4-cells

(b)

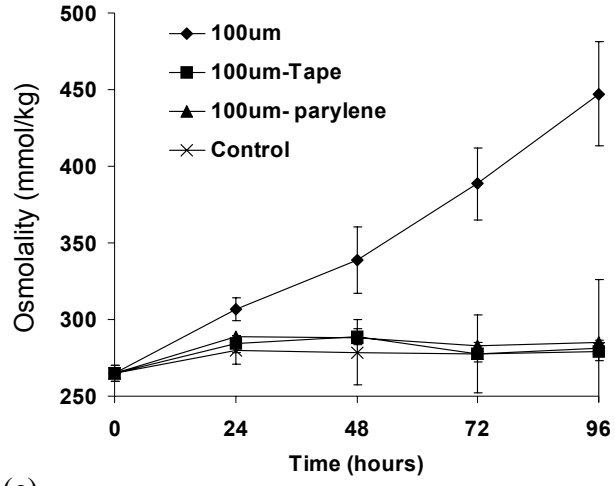
100um
100um-Tape
100um- parylene
Control
Osmolality (mmol/kg)
500
450
400
350
300
250
0
24
48
72
96
Time (hours)

(c)

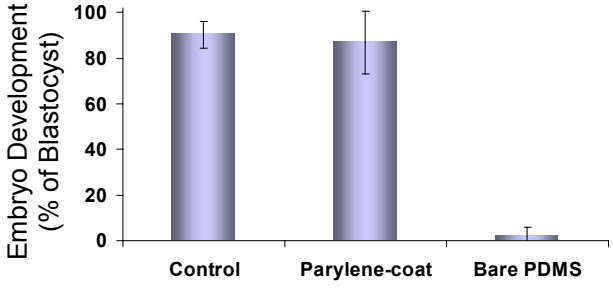
Embryo Development (% of Blastocyst)
100
80
60
40
20
0
Control
Parylene-coat
Bare PDMS

(d)

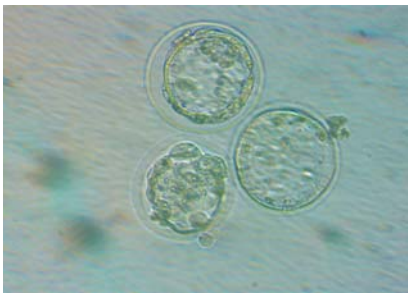

Figure II.4. Microfluidic device for embryo culture. (a) Schematic design of PDMS embryo culture device. (b) Enlarged culture area. It consists of three layers; Upper channel (200μm height) for introducing embryo, middle channel for Braille system (30μm height) and PDMS-parylene-PDMS hybrid membrane with 80μm deep well to keep the introduced embryos in the culture chamber i.e. "Snake head" (300μm wide x 200μm depth).

(a)

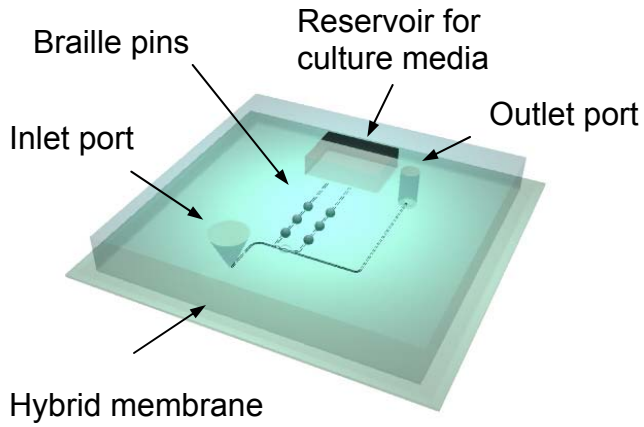
Braille pins
Reservoir for culture media
Outlet port
Inlet port
Hybrid membrane

(b)

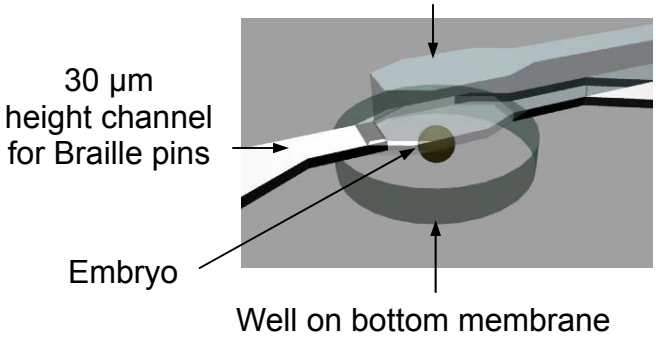
"Snake head" connected to inlet port
30 µm height channel for Braille pins
Embryo
Well on bottom membrane

(c)

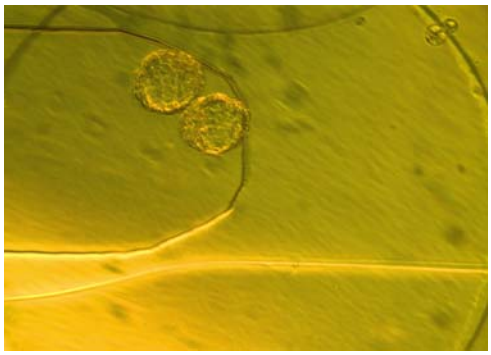

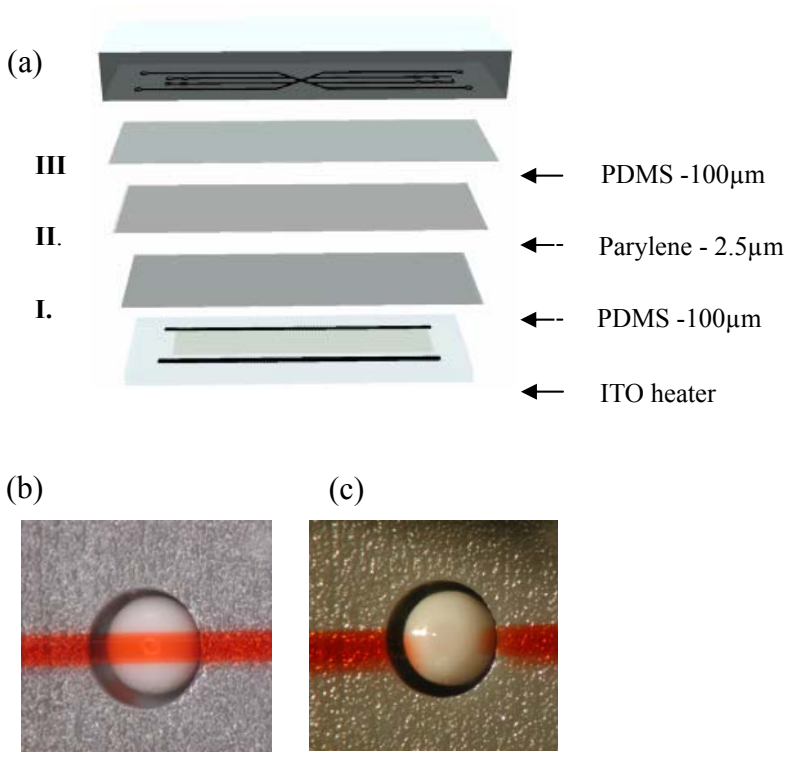

Figure II.5. Schematic representation of Braille display-based microfluidics. A typical design for Braille display-based microfluidics is composed of two layers: Upper bulk PDMS with microchannel and bottom membrane. To test the suitability of the parylene coated PDMS with Braille displays, bottom membrane consists of three layers: 100µm-PDMS, 2.5µm-parylene and 100um-PDMS. For cell culture an ITO heater, composed of a glass slide with ITO thin film (thickness about 1500Å) and aluminum electrodes (thickness about 2000Å) patterned on top of it, is placed underneath the membrane (a). When Braille pin push against the PDMS-Parylene-PDMS hybrid membrane, the channel was fully closed (b). When pin was released, the membrane was restored and channel was opened (c).

Figure II.6. Microfluidic device for HDMEC culture with recirculation. (a) View from the top schematic depicting the location of the Braille pins used for valving and pumping, microfluidic channels, and fluid reservoir. The fluid reservoir has a total volume of ~1 ml and completely surrounds the channel features like a picture frame to provide an unobstructed view of the cells seeded within the channels. Cut-away view shows the location of cells seeded towards the center of the device and recirculation loop with images recorded at the intersection of the "X." (b) Qualitative data showing effects of evaporation on cell viability. Timelapse images for the three experimental conditions for thin membrane: 120 micron, PDMS-only ("thin PDMS," ○), 400 micron, PDMS-only ("thick PDMS" □) and 200 micron, PDMS-parylene hybrid membrane ("hybrid" ◊). Time listed is in minutes. (c) Quantitative data describing effects of evaporation on cell viability. Cell density was normalized to values at T=0.

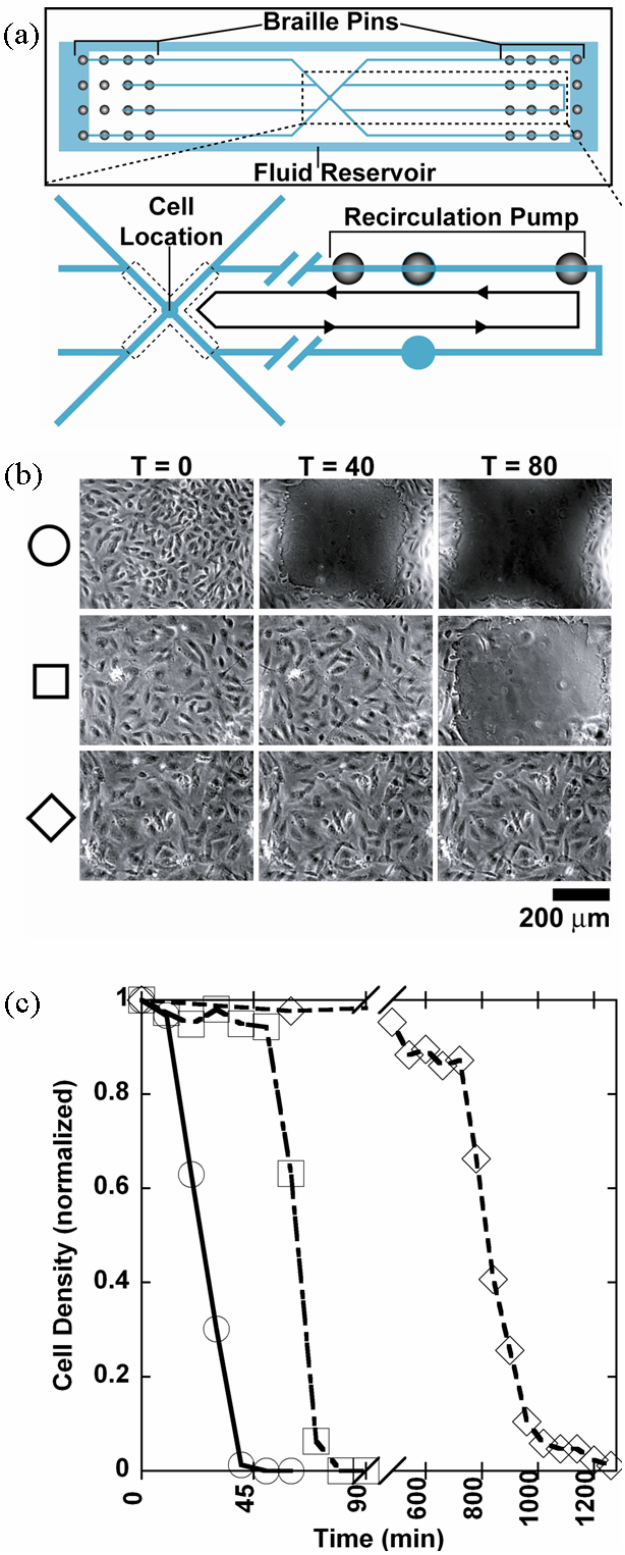
(a)
Braille Pins
Fluid Reservoir
Cell Location
Recirculation Pump
(b)
T = 0
T = 40
T = 80
200 μm
(c)
Cell Density (normalized)
0
0.2
0.4
0.6
0.8
1
0
45
90
600
800
1000
1200
Time (min)

References

[1] Dertinger, S. K. W., Chiu, D. T., Jeon, N. L. & Whitesides, G. M. Generation of gradients having complex shapes using microfluidic networks, *Analytical Chemistry* **73** (6), 1240 (2001).

[2] Figeys, D. & Pinto, D. Lab-on-a-chip: A revolution in biological and medical sciences, *Analytical Chemistry* **72** (9), 330A (2000).

[3] Leclerc, E., Sakai, Y. & Fujii, T. Microfluidic PDMS (polydimethylsiloxane) bioreactor for large-scale culture of hepatocytes, *Biotechnol. Prog.* **20** (3), 750 (2004).

[4] Walker, G. M., Zeringue, H. C. & Beebe, D. J. Microenvironment design considerations for cellular scale studies, *Lab Chip* **4** (2), 91 (2004).

[5] Takayama, S. *et al.* Laminar flows - Subcellular positioning of small molecules, *Nature* **411** (6841), 1016 (2001).

[6] Zhu, X. Y. *et al.* Arrays of horizontally-oriented mini-reservoirs generate steady microfluidic flows for continuous perfusion cell culture and gradient generation, *Analyst* **129** (11), 1026 (2004).

[7] Johnson, T. J., Ross, D., Gaitan, M. & Locascio, L. E. Laser modification of preformed polymer microchannels: Application to reduce band broadening around turns subject to electrokinetic flow, *Analytical Chemistry* **73** (15), 3656 (2001).

[8] Quake, S. R. & Scherer, A. From micro- to nanofabrication with soft materials, *Science* **290** (5496), 1536 (2000).

[9] Duffy, D. C., McDonald, J. C., Schueller, O. J. A. & Whitesides, G. M. Rapid prototyping of microfluidic systems in poly(dimethylsiloxane), *Analytical Chemistry* **70** (23), 4974 (1998).

[10] Moor, A. N., Murtazina, R. & Fliegel, L. Calcium and osmotic regulation of the Na+/H+ exchanger in neonatal ventricular myocytes, *J. Mol. Cell. Cardiol.* **32** (6), 925 (2000).

[11] Zhou, W. C., Chen, C. C., Buckland, B. & Aunins, J. Fed-batch culture of recombinant NS0 myeloma cells with high monoclonal antibody production, *Biotechnol. Bioeng.* **55** (5), 783 (1997).

[12] Ozturk, S. S. & Palsson, B. O. Effect of Medium Osmolarity on Hybridoma Growth, Metabolism, and Antibody-Production, *Biotechnol. Bioeng.* **37** (10), 989 (1991).

[13] Takagi, M., Hayashi, H. & Yoshida, T. The effect of osmolarity on metabolism and morphology in adhesion and suspension chinese hamster ovary cells producing tissue plasminogen activator, *Cytotechnology* **32** (3), 171 (2000).

[14] Lin, J. Q., Takagi, M., Qu, Y. B., Gao, P. J. & Yoshida, T. Enhanced monoclonal antibody production by gradual increase of osmotic pressure, *Cytotechnology* **29** (1), 27 (1999).

[15] Lezama, R., Diaz-Tellez, A., Ramos-Mandujano, G., Oropeza, L. & Pasantes-Morales, H. Epidermal growth factor receptor is a common element in the signaling pathways activated by cell volume changes in isosmotic, hyposmotic or hyperosmotic conditions, *Neurochem. Res.* **30** (12), 1589 (2005).

[16] Wu, M. H., Dirnopoulos, G., Mantalaris, A. & Varley, J. The effect of hyperosmotic pressure on antibody production and gene expression in the GS-NS0 cell line, *Biotechnol. Appl. Biochem.* **40**, 41 (2004).
[17] Brinster, R. L. Studies on Development of Mouse Embryos in Vitro .I. Effect of Osmolarity and Hydrogen Ion Concentration, *J. Exp. Zool.* **158** (1), 49 (1965).
[18] Song, J. W. *et al.* Computer-controlled microcirculatory support system for endothelial cell culture and shearing, *Analytical Chemistry* **77** (13), 3993 (2005).
[19] Urbanski, J. P., Thies, W., Rhodes, C., Amarasinghe, S. & Thorsen, T. Digital microfluidics using soft lithography, *Lab Chip* **6** (1), 96 (2006).
[20] Zheng, B., Roach, L. S. & Ismagilov, R. F. Screening of protein crystallization conditions on a microfluidic chip using nanoliter-size droplets, *J. Am. Chem. Soc.* **125** (37), 11170 (2003).
[21] Koh, C. G., Tan, W., Zhao, M. Q., Ricco, A. J. & Fan, Z. H. Integrating polymerase chain reaction, valving, and electrophoresis in a plastic device for bacterial detection, *Analytical Chemistry* **75** (17), 4591 (2003).
[22] Zhao, Z., Cui, Z., Cui, D. F. & Xia, S. H. Monolithically integrated PCR biochip for DNA amplification, *Sens. Actuator A-Phys.* **108** (1-3), 162 (2003).
[23] Khandurina, J. *et al.* Integrated system for rapid PCR-based DNA analysis in microfluidic devices, *Analytical Chemistry* **72** (13), 2995 (2000).
[24] Lee, D. S. *et al.* Bulk-micromachined submicroliter-volume PCR chip with very rapid thermal response and low power consumption, *Lab Chip* **4** (4), 401 (2004).
[25] Chang, W. J., Akin, D., Sedlak, M., Ladisch, M. R. & Bashir, R. Poly(dimethylsiloxane) (PDMS) and silicon hybrid biochip for bacterial culture, *Biomed. Microdevices* **5** (4), 281 (2003).
[26] Futai, N., Gu, W., Song, J. W. & Takayama, S. Handheld recirculation system and customized media for microfluidic cell culture, *Lab Chip* **6** (1), 149 (2006).
[27] Shin, Y. S. *et al.* PDMS-based micro PCR chip with parylene coating, *J. Micromech. Microeng.* **13** (5), 768 (2003).
[28] Gu W, Zhu X, Futai N, Cho BS & S., T. Computerized microfluidic cell culture using elastomeric channels and Braille displays., *Proc Natl Acad Sci U S A.* **101** (45), 15861 (2004).
[29] Futai, N., Gu, W. & Takayama, S. Rapid prototyping of microstructures with bell-shaped cross-sections and its application to deformation-based microfluidic valves, *Advanced Materials* **16** (15), 1320 (2004).
[30] Mehta, G. *et al.* Quantitative measurement and control of oxygen levels in microfluidic poly(dimethylsiloxane) bioreactors during cell culture, *Biomed. Microdevices* **9** (2), 123 (2007).
[31] Favre, E., Schaetzel, P., Nguygen, Q. T., Clement, R. & Neel, J. Sorption, Diffusion and Vapor Permeation of Various Penetrants through Dense Poly(Dimethylsiloxane) Membranes - a Transport Analysis, *J. Membr. Sci.* **92** (2), 169 (1994).
[32] Watson, J. M. & Baron, M. G. The behaviour of water in poly(dimethylsiloxane), *J. Membr. Sci.* **110** (1), 47 (1996).
[33] Tamai, Y., Tanaka, H. & Nakanishi, K. Molecular Simulation of Permeation of Small Penetrants through Membranes .2. Solubilities, *Macromolecules* **28** (7), 2544 (1995).

[34] Kaplan, A., Jack, R., Opheim, K. E., Toivola, B. & Lyon, A. W., *Clinical Chemistry: Interpretation and Techniques*, 4th ed. (Malvern, PA, 1995).

[35] Barrie, J. A. & Machin, D. Sorption and Diffusion of Water in Silicone Rubbers .1. Unfilled Rubbers, *J. Macromol. Sci.-Phys.* **B 3** (4), 645 (1969).

[36] Annamalai, K. & I., P. K., *Advanced Thermodynamics engineering*. (CRC press, Washington, D.C., 2002).

[37] Du, Y., Mamishev, A. V., Lesieutre, B. C., Zahn, M. & Kang, S. H. Moisture solubility for differently conditioned transformer oils, *IEEE Trns. Dielectr. Electr. Insul.* **8** (5), 805 (2001).

[38] Raty, S. *et al.* Embryonic development in the mouse is enhanced via microchannel culture, *Lab Chip* **4** (3), 186 (2004).

[39] Di Carlo, D., Aghdam, N. & Lee, L. P. Single-cell enzyme concentrations, kinetics, and inhibition analysis using high-density hydrodynamic cell isolation arrays, *Analytical Chemistry* **78** (14), 4925 (2006).

[40] Hubbell, W. H., Brandt, H. & Munir, Z. A. Transient and Steady-State Water-Vapor Permeation through Polymer-Films, *J. Polym. Sci. Pt. B-Polym. Phys.* **13** (3), 493 (1975).

[41] Hayschmidt, A. The Influence of Osmolality on Mouse 2-Cell Development, *J. Assist. Reprod. Genet.* **10** (1), 95 (1993).

[42] Randall, G. C. & Doyle, P. S. Permeation-driven flow in poly(dimethylsiloxane) microfluidic devices, *Proceedings of the National Academy of Sciences of the United States of America* **102** (31), 10813 (2005).

[43] Verneuil, E., Buguin, A. & Silberzan, P. Permeation-induced flows: Consequences for silicone-based microfluidics, *Europhys. Lett.* **68** (3), 412 (2004).

CHAPTER III

Dynamic Microfunnel Culture Enhances Embryo Development and Pregnancy Rates

Despite advances in *in vitro* manipulation of pre-implantation embryos, there is still a lag in the quality of embryos produced *in vitro* leading to lower pregnancy rates compared to embryos produced *in vivo.* We hypothesized that a dynamic microfunnel embryo culture system would enhance outcomes by better mimicking the fluid mechanical stimulation and chemical agitation embryos experience *in vivo* from ciliary currents and oviductal contractions. Indeed, using a mouse embryo model, average cell counts for blastocysts after 96 hours of culture in dynamic microfunnel conditions increased 70% over that of conventional static cultures. Importantly, the dynamic microfunnel cultures significantly improved embryo implantation and ongoing pregnancy rates over static culture to a level that approached that of *in utero*-derived preimplantation embryos. The improved pregnancy outcomes along with the simple and user-friendly design of the microfunnel system has potential to alleviate current inefficiencies in embryo production for biomedical research, genetic gain in domestic species, and fertility treatment in humans.

Introduction

Since the first *in vitro* development of fertilized mouse ova on a blood clot in the presence of oviduct tissue in 1941, extensive research has been undertaken to improve mammalian preimplantation embryo development in culture. Most studies have focused on modifications of soluble media components such as salts, energy or nitrogen sources, and growth factor / hormone supplementation in attempts to improve embryo development[1]. Nevertheless embryos derived from current culture conditions lag behind those derived from *in vivo* microenvironments of the oviduct and/or uterus in regard to embryo development, implantation, and subsequent pregnancy. Contemporary *in vitro* fertilization (IVF) procedures entail gamete isolation, fertilization, and embryo culture in dishes, test tubes or microdrops using media volumes of 10-1000 microliters under substantially static conditions[2,3]. Conversely, *in vivo* embryos develop from the zygote to blastocyst stage during a period of transit through the oviduct, where they reside spatially juxtapositioned between epithelial cells within luminal crypts representing a moist microenvironment[4]. During most of this time, embryos experience dynamic mechanical[5] and chemical conditions[6]. Segmental muscular contractions in the oviduct are presumed to agitate tubal contents[7] while oviductal epithelial cells contribute to ciliary currents[8,9], which collectively exert pulsatile fluid and solid mechanical forces on embryos[10,11]. We hypothesized that reproducing an aspect of these dynamic conditions *in vitro* would enhance embryo development and thus improve pregnancy rates.

Previously, static microfluidic culture systems with sub-microliter effective culture volumes[12] have been reported to enhance development rates presumably due to enhanced

embryo self-conditioning of the very small volumes of culture media. This microfluidic system, however, has not yet been shown to enhance pregnancy rates. Dynamic microfluidic culture systems with continuous perfusion were also examined[13] but with poor embryo development across a range of flow rates. Continuous flow microchannel systems may exert beneficial fluid mechanical stimulations to embryos, but only at the cost of washing out growth-promoting autocrine factors [14,15]. An oil suspended microdrop with internal media recirculation has also been used for embryo culture[16]. In this system, autocrine factors are retained but the device configuration only allowed for exposure of embryos to a shear stress level (1.2 dynes/cm^2) that is orders of magnitudes higher than is physiological and resulted in upregulation of stress signaling pathways and embryo death. We thus hypothesized that what is necessary to better mimic the dynamic microenvironment that exists *in vivo* is to enable physiological levels of fluid mechanical stimulation yet with retention of a significant portion of autocrine factors which are known to benefit embryo development[17].

Methods

Microfunnel fabrication. Relief features of desired channel structures were composed of SU-8 (MicroChem, Newton, MA) and fabricated on a thin glass wafer (200μm thick) by using backside diffused-light photolithography[18]. A thick (~ 8mm) PDMS (Sylgard 184, Dow-Corning at a 1:10 curing agent-to-base ratio) slab with funnel and channel features[19] were created by casting PDMS prepolymer against the SU-8 features and curing at 60°C for 120 min and at 120°C for 30 min. The resulting PDMS slab was attached to a thin PDMS-parylene-PDMS hybrid membrane[20].

Fluid Actuation. On-chip peristaltic pumping was performed using multiple computer-controlled, piezoelectric, movable pins on a commercial Braille display (Sighted Electronics, Inc, NJ).[21]

Embryo preparation and implantation. All animal procedures were approved by the University of Michigan Animal Care and Use Committee. Denuded zygotes[22] from B6C3F1 females were randomly distributed into 10µl of Potassium Simplex Optimized Medium (KSOM; Specialty Media, Phillipsburg, NJ) and overlaid with mineral oil in microfluidic devices with dynamic media flow or in static culture drops in a humidified environment of 5% CO_2, 20% O_2 and balance N_2 at 37°C. *In vivo* control embryos were collected from uteri corresponding to 72h or 96h culture. In some studies embryos were transferred to oviducts of (C57BL/6 X DBA/2) F1 mice (-0.5d asynchronous). Treatments were allocated in groups of 7 embryos to each uterine horn according to stage of embryo development starting from the seven furthest advanced to the seven least advanced stage embryos. This resulted in the 7 best embryos from dynamic culture being transferred to one recipient uterine horn and the 7 best embryos from static culture into the recipient's contra lateral horn. After 15d gestation, hysterectomy was performed to evaluate and quantify embryo implantation sites and ongoing pregnancies. Fetal weight, stage of development and normalcy were also analyzed. Parametric and nonparametric data were analyzed with ANOVA/unpaired t-test and χ-square statistics, respectively. All animal procedures were approved by the University of Michigan Animal Care and Use Committee.

Design of 3D mesh geometries used in Fluent simulation. Microdrop in an organ dish: The liquid drop is assumed to be a hemisphere with a radius of 1.68mm calculated by

the drop having a total volume of 10µl of media covered by oil. The embryo is approximated to be a sphere with a 50µm radius at the center of the hemisphere. Microchannel (Straight microfluidic channel with barrier): The channel dimensions are 1.5mm in length, 1mm in width, and 0.25mm in height as previously designed by a reference group. The barrier has a cross-section 0.1 mm in width and 0.11 mm in height (longitudinal cut of the channel) and placed in the middle of channel. The sphere, acting as an embryo, was placed in front of the barrier with a 10µm gap. Microfunnel: The funnel has a 0.25mm bottom radius, 1.77mm top radius, and 2.63mm height. Funnel dimensions were calculated based on the 10µl volume of media and 60° angle of the funnel wall in respect to the bottom channel. The funnel and a 50µm radius sphere are located at the middle of a straight channel with dimensions of 1.5mm in length, 0.4mm in width and 0.03mm in height. Each sphere has a 10µm gap from its respective bottom boundary. For microdrop and microfunnel the interfaces between media and covered oil were considered as walls for simulation purposes. The computational meshes consist of 59,856 elements, 181,202 elements and 55,765 elements for microdrop, microchannel and microfunnel, respectively and the results are mesh-independent.

Embryo secretion and volumetric source of species. Assuming embryo secretes factors with a constant production rate over culture periods and the transport of the factors in media depends on mass diffusion in the absence of flow in media, the secretion rate from embryo can be modeled as the specified species mass production rate at wall or surface of embryo, in computer simulation with Fluent. Here, a volumetric source term ($kg/m^3 \cdot sec$) of a species in a fluid zone was defined only in the cells adjacent to the spherical wall (embryo) by using a user defined function (UDF). In this simulation, the properties of epidermal growth factor (EGF) are chosen as the representatives for beneficial factors. EGF has a

molecular weight, 6045 and diffusion coefficient, D_{12}= 1.66·E-10. In UDF, a constant mass production rate of EGF, 1.68E-15 [kg/s] was assigned and a volumetric source (kg/m^3·sec) was obtained by dividing the production rate by volume of cell. A waste product such as ammonia showed similar retention ratios as EGF for the three conditions simulated (data not shown here). While thirteen to fifteen embryos were placed in each condition, simulation was done with single embryo. Because we used normalized values of concentration for comparison of three different conditions, a single embryo model is adequate for comparisons.

Sampling volume. The "sampling volume" is the volume within which ligands are accessible for binding by receptors on an embryo. To determine a relevant sample volume, we considered the average distance, l, from within which an embryo can sample ligands. This distance can be approximated as $(D_L/k_r)^{1/2}$, where D_L is the translational diffusion coefficient of the ligand and k_r is the dissociation rate constant of the receptor for this ligand[23]. In the case of epidermal growth factor (EGF) which characteristic parameters are used in simulation and is known to be a relevant growth factor for embryo development, D_L is 1.66·E-10 [m^{2}s^{-1}][24] and k_r is 5.7E-3[s^{-1}][23]. Thus l is approximately 171μm. For other molecules such as insulin-like growth factor-I (IGF-I) with D_L=1.59E-10 [m^{2}s^{-1}][25] and k_r =1.7E-3[s^{-1}][26], l is approximately 306μm. From these estimates, we used ~250μm as a characteristic distance of interest to determine a sampling volume for comparison.

Results and Discussion

The microfunnel culture system was constructed of poly(dimethylsiloxane) (PDMS) and cultured embryos in a ~500 micrometer diameter, flat, optically transparent floor (Figure III. 1a). The microfunnel was connected to microchannels that provided periodic fluid pulses of media at physiological frequencies (0.135 Hz in rabbit oviduct[27]). These channels were thin (30 micron high) and wide (400 micron wide) to prevent embryos from entering and to enable peristaltic fluid pumping by deformation of the channels using computer controlled piezoelectric pins. The microfunnel had four functions: i) It localized multiple embryos to a small region (~500 micron diameter); ii) It provided a fluid reservoir (up to tens of microliters) that mimicked the characteristic dimensions (millimeters) of the oviduct and buffered the chemical exchange rate in the fluid environment of the embryo; iii) It modulated the fluid mechanical stimulation to which embryos were exposed by fluid flow from the microchannels; iv) It provided a practical design where by embryos were easily loaded and unloaded by simple pipetting.

Biologic enhancement of the dynamic microfunnel culture was examined in a mouse model. Denuded pronuclear-stage zygotes from B6C3F1 females were cultured under three different conditions (13~15 zygotes per condition per replicate): microdrop culture in culture dishes (Microdrop-control), static microfunnel culture (Microfunnel-control), and dynamic microfunnel culture with flow-through of fluid at a pin actuation rate of 0.1Hz (Microfunnel-pulsatile) (Figure III. 1b). As an *in vivo*-control, embryos were collected from uteri temporally corresponding to culture-derived embryos. The total number of blastocysts developed from zygotes over a 96h culture period was not significantly different between culture conditions. Blastocyst developmental stage obtained, however, was significantly enhanced ($P<0.01$) under dynamic microfunnel culture conditions as evidenced by larger

numbers of hatching or hatched blastocysts (Microdrop-control 31%; Microfunnel-control 23%; Microfunnel-pulsatile 71%) and significantly higher ($P<0.01$) average number of cells per blastocyst (Microdrop-control 67±3; Microfunnel-control 60±3; Microfunnel-pulsatile 109±5) as shown in Figure III. 2a,b. Blastocyst cell numbers in dynamic microfunnel cultures (109±5) more closely recapitulate numbers obtained from *in vivo*-grown blastocysts (144±9) (Figure III. 2b). Importantly, the enhanced embryo development enabled by the dynamic microfunnel cultures led to correspondingly higher rates of implantation, lower rates of abortion, and significantly higher on-going pregnancy rates compared to embryos cultured in static microdrops ($P<0.05$) as shown in Figure III. 2c. Fetuses originating from dynamic microfunnel culture demonstrated normal development as assessed by developmental age, fetal weight, and placental weight.

To determine if enhanced embryo development in the dynamic microfunnel systems is time or stage dependent, we systematically varied the duration and developmental-stage at which embryos cultured in microfunnels were exposed to dynamic culture conditions (Figure III. 2d). Embryos in microfunnels were cultured under dynamic conditions for 48hr at the beginning, 48 hrs at the end, or 96 hours and compared with embryos under static condition over the entire 96hrs. The developmental rate observed was proportional to the duration of dynamic culture regardless of the stage of embryo development. Thus, embryos cultured under dynamic conditions for 48h had similar significantly enhanced development and cell numbers at 96h compared to static controls ($P<0.01$) regardless of whether the 48h period was at the beginning or end of the 96h.

The differences in embryo culture microenvironments are highlighted by computational simulations (Fluent, www.fluent.com; Figure III. 3). Three different 3D-meshes were modeled based on actual geometries: Microdrop with 10µl media, Microchannel with barrier and a Microfunnel. In each simulation, an embryo was modeled to secrete an autocrine factor for 48 hrs resulting in formation of a concentration gradient in its vicinity. Here it is useful to consider a sampling volume in the vicinity of the embryo (~250 micron radius region around an embryo) with which to compare the effective autocrine concentration in each device setting. For the microchannel and microfunnel, fluid flow was also simulated with average inlet flow velocities that correspond to the experimentally used values. The simulations show that conventional microdrop cultures retain most of the autocrine factors produced by the embryo, but exert negligible fluid mechanical stimulation. The continuous perfusion microchannel culture provides fluid mechanical stimulation that may be beneficial to the embryo but the flow also removes most of the beneficial autocrine factors. Importantly, the dynamic microfunnel system can provide benefits of both fluid mechanical stimulation to the embryo and retention of significant amounts of autocrine factors simultaneously (Figure III. 3).

Conclusion

Here, we demonstrated that even when starting with the same media, gaseous environment, and initial embryo quality, significant enhancements in embryo development and fetus production can be achieved by dynamic microfunnel culture. The portable

computerized microfluidic systems described are designed to be readily manipulated by researchers and clinical biologists using conventional pipettes, incubators, and microscopes. The user-friendly system architecture, flexibility in microchannel and chip design, and programmability of the fluid actuation system allows convenient and practical manipulation of chemical and mechanical microenvironment for *in vitro* embryo production. Improved pregnancy outcomes can alleviate current inefficiencies in embryo production for biomedical research, genetic gain in domestic species, and fertility treatment in humans. Combining physiological mechanical stimulation with retention of beneficial autocrine factors may also benefit a broad range of cell culture technologies beyond the dynamic microfunnel embryo culture systems described here.

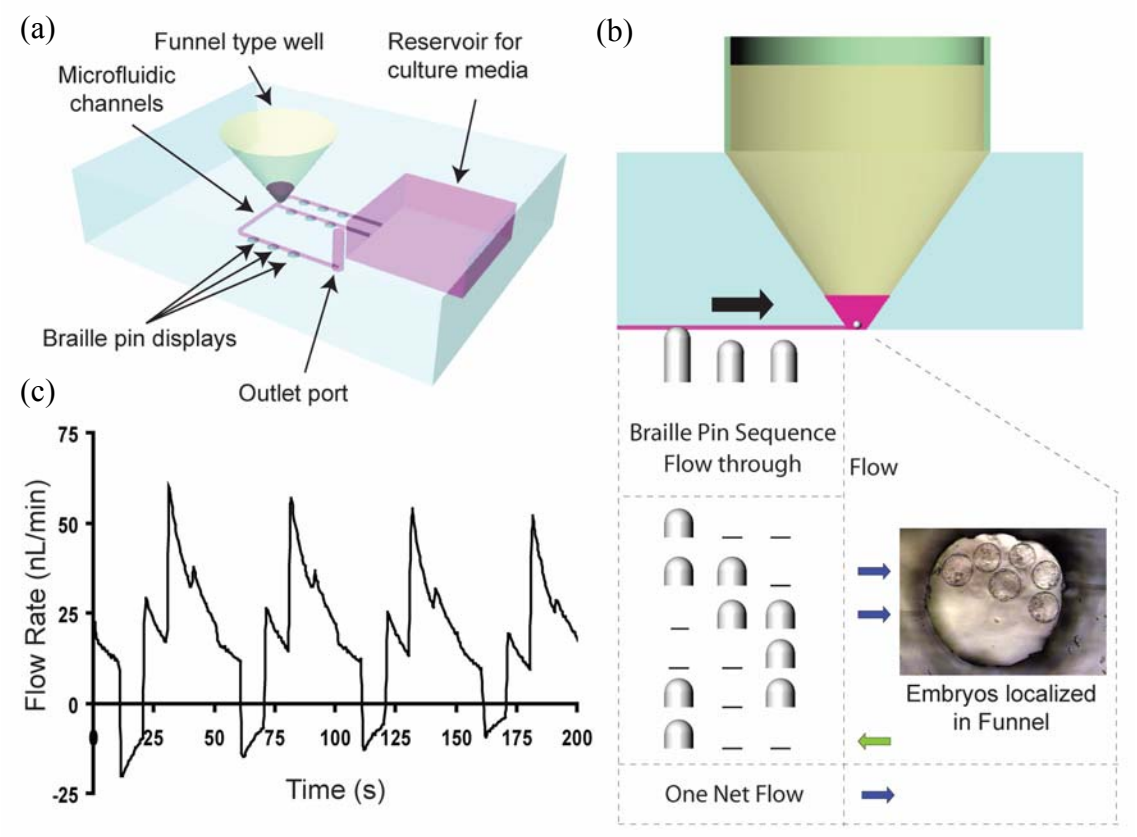

Figure III.1. Dynamic microfunnel culture device and flow pattern. a) Schematic drawing of a microfunnel device. The device is placed on an array of piezoelectric pin actuators provided by Braille displays. b) Embryos are loaded and cultured in the microfunnel under the flow-through condition created by the pin actuation sequence. c) The flow rate generated over four cycles of the five-step Braille pin actuation sequence at 0.1Hz was measured by a digital flow meter (SLC1430, http://www.sensirion.com). The average flow rate of 17.9 nL/min was used as the inlet velocity for FLUENT simulations in Figure III. 3.

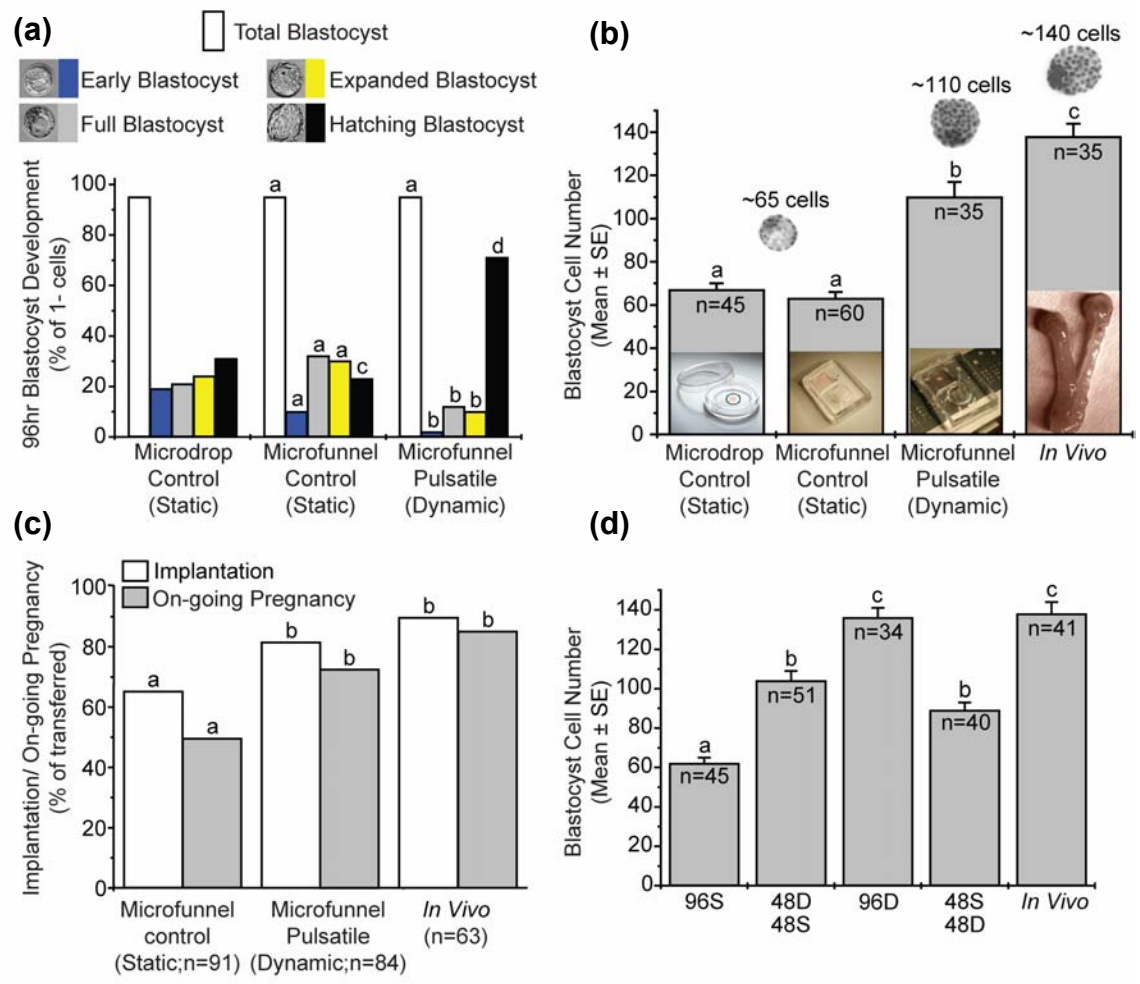

Figure III.2. Dynamic microfunnel culture enhances blastocyst development and implantation. a) Blastocysts obtained in each culture condition were morphologically categorized into four different stages: Early, Full, Expanded, and Hatching Blastocysts. Blastocyst development to each stage was not significantly different between static culture comparisons, thus subsequent statistical comparisons were performed between microfunnel-control (static) and microfunnel-pulsatile (dynamic). Blastocysts derived under microfunnel-pulsatile culture conditions developed faster than those from static conditions. Different letters between culture treatments within a stage of blastocyst development represent a significant difference between the microfunnel–control and microfunnel-pulsatile (a,b= $p<0.05$; c,d = $p<0.01$). b) Dynamic chip condition (microfunnel-pulsatile) shows a greater number of cells per blastocyst compared to static culture, with results closer to *in vivo* conditions (a,b,c = $p< 0.01$). c) Comparison of percentage of static, dynamic and *in vivo* grown and transferred embryos that implanted and maintained normal on-going pregnancies at 15 days post transfer. Different superscripts indicate statistical significance (a,b = $p<0.05$). d) Effect of duration and timing of dynamic culture on embryo development. Mean blastocyst cell counts from embryos cultured for 96 hours under varying culture conditions of either dynamic or static media flow. Different superscripts ^{a,b} indicate statistical significance ($p<0.05$). Culture conditions of either dynamic or static media flow were interchanged at 48 hour increments.

Figure III.3. Dynamic microfunnel culture provides fluid mechanical stimulation with retention of autocrine factors. Summary of flow pathlines, mechanical stimulation, and autocrine factor distribution/retention provided by different embryo culture methods as simulated using Fluent. Microdrops retain autocrine factors but do not provide mechanical stimulation. Microchannels provide mechanical stimulation but do not retain autocrine factors. Dynamic microfunnel cultures provide both. Flow pathline: pathlines on the longitudinal plane for the channel and funnel. Pathlines represent the lines travelled by neutrally buoyant particles in equilibrium with the fluid motion. Within the straight micro-channel the pathlines predominantly pass over the embryo and barrier washing away embryo secreted factors. Pathlines within the micro-funnel design show a vortex effect in the middle of the funnel which helps retain autocrine factors secreted from embryos. Autocrine factor distribution: Concentration gradient formed within devices in the presence of an embryo secreting an autocrine factor at a constant physiological rate for 48 hrs. The normalized minimum value, zero is colored with Blue and the normalized maximum value, one, is colored with Red on the color scale. The average concentration of autocrine factor in a sampling volume for the straight channel culture dramatically dropped to below 2% of the level found for the microdrop culture. Conversely, the funnel shaped culture retained 40% of the level found for the microdrop culture in the same sampling volume. Scale bar = 100 microns. Mechanical stimulation on embryo: shear stress experienced by the simulated embryo. Minimum shear stress, zero is colored with Blue and maximum value, 7E-3 (dyn/cm^2), is colored with Red on the color scale. Here, the maximum instantaneous velocity (6.86E-3cm/s) in Figure III. 1c and the velocity (5.56E-4cm/s) equivalent to a flow rate of 5 μl/hr are applied at inlet for microfunnel and microchannel, respectively. The average shear forces per area are 1.99E-3 dyn/cm^2 for microchannel and 3.55E-3 dyn/cm^2 for microfunnel.

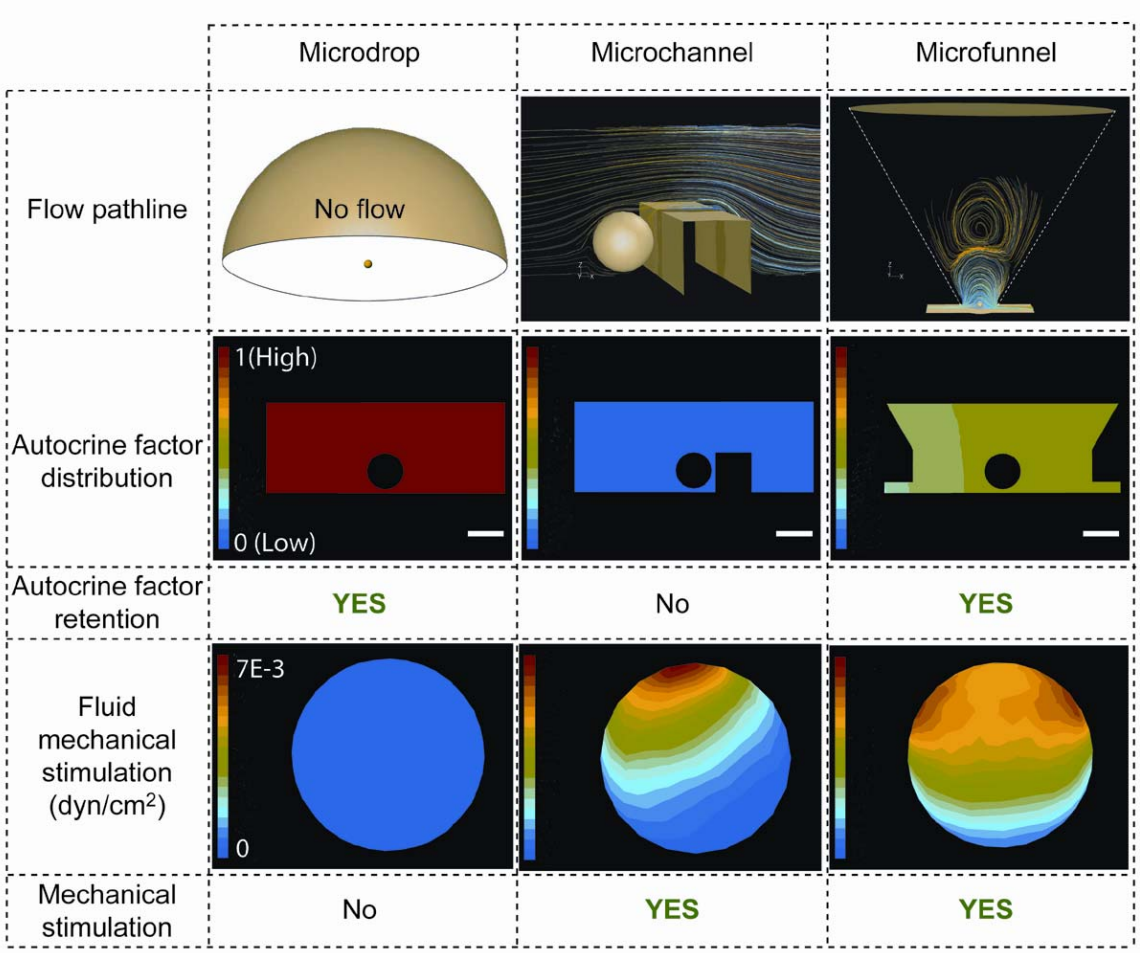
Microdrop
Microchannel
Microfunnel
Flow pathline
No flow
Autocrine factor distribution
1(High)
0 (Low)
Autocrine factor retention
YES
No
YES
Fluid mechanical stimulation (dyn/cm2)
7E-3
0
Mechanical stimulation
No
YES
YES

References

[1] Loutradis, D. *et al.*, in *Young Woman at the Rise of the 21st Century: Gynecological and Reproductive Issues in Health and Disease* (2000), Vol. 900, pp. 325.

[2] Thompson, J. G. Culture without the petri-dish, *Theriogenology* **67** (1), 16 (2007).

[3] Trounson, A. O. & Gardner, D. K., *Handbook of in vitro fertilization* 2nd ed. (CRC Press LLC, Boca Raton, 2000).

[4] Leese, H. J., Tay, J. I., Reischl, J. & Downing, S. J. Formation of Fallopian tubal fluid: role of a neglected epithelium, *Reproduction* **121** (3), 339 (2001).

[5] Fauci, L. J. & Dillon, R. Biofluidmechanics of reproduction, *Annual Review of Fluid Mechanics* **38**, 371 (2006).

[6] Hardy, K. & Spanos, S. Growth factor expression and function in the human and mouse preimplantation embryo, *J. Endocrinol.* **172** (2), 221 (2002).

[7] Muglia, U. & Motta, P. M. A new morpho-functional classification of the Fallopian tube based on its three-dimensional myoarchitecture, *Histol. Histopathol.* **16** (1), 227 (2001).

[8] Gaddumro.P & Blandau, R. J. In-Vitro Studies on Ciliary Activity within Oviducts of Rabbit and Pig, *Am. J. Anat.* **136** (1), 91 (1973).

[9] Talbot, P., Geiske, C. & Knoll, M. Oocyte pickup by the mammalian oviduct, *Mol. Biol. Cell* **10** (1), 5 (1999).

[10] Anand, S. & Guha, S. K. Mechanics of Transport of Ovum in Oviduct, *Med. Biol. Eng. Comput.* **16** (3), 256 (1978).

[11] Blake, J. R., Vann, P. G. & Winet, H. A Model of Ovum Transport, *Journal of Theoretical Biology* **102** (1), 145 (1983).

[12] Raty, S. *et al.* Embryonic development in the mouse is enhanced via microchannel culture, *Lab Chip* **4** (3), 186 (2004).

[13] Hickman, D. L., Beebe, D. J., Rodriguez-Zas, S. L. & Wheeler, M. B. Comparison of static and dynamic medium environments for culturing of pre-implantation mouse embryos, *Comparative Medicine* **52** (2), 122 (2002).

[14] Paria, B. C. & Dey, S. K. Preimplantation embryo development in vitro: cooperative interactions among embryos and role of growth factors., *Proc Natl Acad Sci U S A.* **87** (12), 4756 (1990).

[15] Walker, G. M., Zeringue, H. C. & Beebe, D. J. Microenvironment design considerations for cellular scale studies, *Lab Chip* **4** (2), 91 (2004).

[16] Xie, Y. F. *et al.* Shear stress induces preimplantation embryo death that is delayed by the zona pellucida and associated with stress-activated protein kinase-mediated apoptosis, *Biology of Reproduction* **75** (1), 45 (2006).

[17] Oneill, C. Evidence for the requirement of autocrine growth factors for development of mouse preimplantation embryos in vitro, *Biology of Reproduction* **56** (1), 229 (1997).

[18] Futai, N., Gu, W. & Takayama, S. Rapid prototyping of microstructures with bell-shaped cross-sections and its application to deformation-based microfluidic valves, *Advanced Materials* **16** (15), 1320 (2004).

[19] Duffy, D. C., McDonald, J. C., Schueller, O. J. A. & Whitesides, G. M. Rapid prototyping of microfluidic systems in poly(dimethylsiloxane), *Analytical Chemistry* **70** (23), 4974 (1998).

[20] Heo, Y. S. *et al.* Characterization and resolution of evaporation-mediated osmolality shifts that constrain microfluidic cell culture in poly(dimethylsiloxane) devices, *Analytical Chemistry* **79** (3), 1126 (2007).

[21] Gu, W., Zhu, X. Y., Futai, N., Cho, B. S. & Takayama, S. Computerized microfluidic cell culture using elastomeric channels and Braille displays, *Proceedings of the National Academy of Sciences of the United States of America* **101** (45), 15861 (2004).

[22] Hogan, B., Beddington, R., Costantini, F. & Lacy, E., *Manipulating the Mouse Embryo*, 2nd ed. (Cold Spring Harbor Laboratory Press, Plainview, New York, 1994).

[23] Lauffenburger, D. A. & Linderman, J. J., *Receptors:Models for binding, trafficking, and signaling*. (Oxford University Press, New York, 1993).

[24] Thorne, R. G., Hrabetova, S. & Nicholson, C. Diffusion of epidermal growth factor in rat brain extracellular space measured by integrative optical imaging, *J. Neurophysiol.* **92** (6), 3471 (2004).

[25] Nauman, J. V., Campbell, P. G., Lanni, F. & Anderson, J. L. Diffusion of insulin-like growth factor-I and ribonuclease through fibrin gels, *Biophys. J.* **92** (12), 4444 (2007).

[26] Jansson, M. *et al.* Characterization of ligand binding of a soluble human insulin-like growth factor I receptor variant suggests a ligand-induced conformational change, *J. Biol. Chem.* **272** (13), 8189 (1997).

[27] Bourdage, R. J. & Halbert, S. A. Invivo Recording of Oviductal Contractions in Rabbits During the Periovulatory Period, *American Journal of Physiology* **239** (3), R332 (1980).

CHAPTER IV

Real Time Culture and Analysis of Single Embryo Metabolism using Innovative Microfluidic Device with Deformation-Based Actuation

Introduction

In United States (US) and around the world, 13-18% of couples have infertility problems. Treatments such as in vitro fertilization (IVF) is available people still struggle with low success rates (~ 30% in US) at an average cost of $12, 400 per cycle in the US. To improve the success rate, multiple embryos (3~5) are transferred, which causes high multiple pregnancy rates and subsequent higher pregnancy complications. For example, the perinatal mortality for triplets is eightfold greater than that of singletons[1]. Thus, reducing the incidence of high-order multiple pregnancies while maintaining an overall high IVF success rate is a major goal of human IVF. Achieving single embryo transfer with high success is still challenge, at least in part, because it is difficult to obtain high quality embryo and to select the one best embryo for implantation.

Current IVF methodologies employ only morphological characteristics such as cleavage rate and cell number for determining which embryos are suitable for implantation[2,3]. This scoring system is, however, notoriously difficult and subjective. What is required to increase pregnancy rates without increasing the risk of multiple pregnancies is the improvement of in vitro culture methods to provide higher quality embryos together with development of reliable methods to identify the highest quality preimplantation embryo from

a group of morphologically similar ones so that only one, high quality embryo has to be implanted.

Methods of predicting and quantifying embryo viability have been discussed extensively[4]. Parameters for consideration include assessment of morphology[5,6], development in culture[7], production of soluble human leukocyte antigen-G (sHLA-G)[8], oxygen uptake measurements[9,10], amino acid metabolism[11,12] and nutrient uptake measurements[13]. The ability to predict whether an embryo will develop in culture has been associated with rate of cleavage in animal studies[7]. It was observed that the speed at which an embryo developed was related to its ability to form a blastocyst. Furthermore, morulae and blastocysts which developed from slowly dividing embryos gave rise to lower fetal development after transfer than those embryos which developed from more rapidly dividing cleavage stages[7]. Similarly, Shoukir *et al.*[14], have observed that those embryos forming blastocyst earlier are more viable. Amino acids secreted and taken up by human embryos during different stages are also correlated to blastocyst development. Brison *et al.*[11] examined the changes in the concentration of amino acids secreted by human embryos and reported an association between decreased glycine and leucine, and increased asparagine levels in culture media and clinical pregnancy and live birth. One of most reliable criterion for the quantification of embryo viability is energy metabolism, which can be measured non-invasively for individual embryos in culture[15]. Lane et al.[4], used both glucose uptake and lactate production (to estimate glycolytic activity) to select prospectively individual day-4 mouse blastocysts for transfer. Mouse blastocysts with low (normal) glycolytic activity had a significantly higher viability than those with elevated levels of glycolysis. Furthermore, the

use of glycolytic activity as a selection marker resulted in a four-fold increase in pregnancy rates. More recently, Gardner *et al*.[16] reported that glucose consumption in day-4 human embryos that went on to form blastocysts was twice as high compared to those that did not. Furthermore, they determined that poor quality blastocysts consumed significantly less glucose than the highest grade embryos. Such data therefore supports that it is possible to select embryos for transfer using metabolic criteria. Although the metabolic criteria are present to evaluate the embryo viability, the application of these methodologies to clinical use has been limited because of the requirement of dedicated equipment, a technical staff that would be costly and a lack in the speed to allow the information to be used clinically in the limited window of time acceptable for embryo transfer[13]. Thus, a validated technology that predicts reproductive potential of embryos through a rapid, noninvasive method is necessary for clinical applications.

The advent of microfluidics has opened the avenue to developing experimental platforms for manipulating and analyzing chemical and biological systems that necessitate exquisite control of chemical concentrations, spatial resolution, and temporal resolution[17]. Microfluidic devices have attracted the attention of many researchers due to their speed, simplicity, small reagent consumption and selectivity in handling fluids in order to deliver many chemical and biochemical components through a complex network[18]. Specifically, one of the main reasons for the researcher's interest in microfluidic devices is that several functionalities can be integrated into a single microchip, which makes the lab-on-a chip technology a reality[19].

In this chapter, we utilized glucose consumption as a measure of embryo metabolism. A microfluidic assay for this biomarker was integrated into a microfluidic embryo culture

system to assess preimplantation embryo health so that the one best embryo can be selected and eventually transferred.

Methods

Glucose measurements. A convenient one-step method for quantifying glucose is to use a coupled glucose oxidase - peroxidase mediated reaction to generate red-fluorescent resorufin from colorless Amplex Red reagent (10-acetyl-3,7-dihydroxyphenoxazine; Molecular Probes; www.probes.com). In this assay, glucose oxidase (Sigma; www.sigmaaldrich.com) catalyzes the conversion of lactate to pyruvate and H_2O_2. In the presence of horseradish peroxidase (HRP; Sigma), the H_2O_2 thus generated then reacts with the Amplex Red reagent in a 1:1 stoichiometry to generate red-fluorescent resorufin. The high extinction coefficient (54,000 cm-1M-1) and the long emission wavelengths (587 nm) allow sensitive fluorescent quantification of glucose with little interference from the autofluorescence found in culture media.

Device Fabrication for Microfluidic Endothelial Cell Culture. The Microfluidic device (Figure IV. 1) was composed of a thick (~ 8mm) PDMS slab with microfluidic channel features, fabricated by using soft lithography[20], attached to a PDMS-parylene-PDMS hybrid membrane[21]. The thick PDMS slab with channel features was prepared by casting prepolymer (Sylgard 184, Dow-Corning) at a 1:10 curing agent-to-base ratio against positive relief features. The relief features were composed of SU-8 (MicroChem, Newton, MA) and fabricated on a thin glass wafer (200μm thick) by using backside diffused-light

photolithography[22]. The prepolymer was then cured at 60°C for 60 min, and holes were punched in it by a sharpened needle. The PDMS-parylene-PDMS hybrid membrane was prepared by the following stepwise procedure: spin coating PDMS onto a 4″ silanized silicon wafer to a thickness of 100 μm, curing this layer at 120°C for 30 min, depositing a 2.5 or 5 μm thick parylene layer using a PDS 2010 labcoater, plasma oxidizing the resulting parylene surface for 90 seconds, and spin coating another 100 μm thick layer of PDMS and curing to get a total thickness of ~200 μm.

Indium tin oxide (ITO) Heater. The ITO heater was constructed by an ITO layer deposited on a glass slide with metallic films for electric contact. First, the glass slide was masked using scotch tape to form the pattern for the ITO layer. In order to smoothly generate electric current through the ITO layer for uniform joule heating, two aluminum strips (1 mm width and 2000Å thick) were patterned and coated in a similar manner on two edges of the ITO layer. Electrical wires were attached to the aluminum stripes using silver epoxy glue to form connections to external control circuits. A commercially available wire thermocouple (5TC-TT-J; Newport, Santa Ana, CA) was attached onto the heater surface for temperature sensing. All the wires were connected to a microprocessor based temperature control unit (CT16A2088, Minco Products, Inc., Minneapolis, MN) for feedback control of the heater surface temperature. As a result, the heater surface can be maintained constantly at desired temperature.

Fluid Actuation for assay. Experiments were conducted on the stage of an inverted microscope (Nikon TS-100F, Japan), imaged with a 10x Ph1 objective (Achromat), and

recorded using Coolsnap CF2 Camera with MetaVue software. To account for the lack of controlled temperature and 5% CO_2 tension provided by a cell culture incubator, the bottom of the PDMS device was heated to 37°C (ITO heater, PID Temperature Controller, Minco, Minneapolis, MN). Braille pins were reconfigured via computer-control for introduction of the three reagents into a mixing channel, then valving for enzyme reaction, and finally pushing the mixed plug in the mixing channel towards a detection zone for measurement of intensity and finally a waste reservoir.

Embryo preparation. Six- to eight-week-old B6C3F1 female mice (Charles River) were superovulated by an intraperitoneal administration of 10 IU of pregnant mare serum gonadotropin (PMSG; Sigma Chemical Co.) by injection, followed 44h later with an injection of 10 IU human chorionic gonadatropin (hCG; Sigma Chemical Co.). Denuded zygotes[23] from B6C3F1 females were randomly distributed into 10µl of Potassium Simplex Optimized Medium (KSOM; Specialty Media, Phillipsburg, NJ) and overlaid with mineral oil in microfluidic devices with dynamic media flow or in static culture drops in a humidified environment of 5% CO_2, 20% O_2 and balance N_2 at 37°C. *In vivo* embryos were collected from uteri corresponding to 72h or 96h culture. All animal procedures were approved by the University of Michigan Animal Care and Use Committee.

Results and Discussion

Biochemical methods for embryo analysis based on measurement of metabolic rates do exist, but are not practical for clinical use because of the difficulty in manipulating precise

amounts of sample and reagents at the sub-microliter scale. Here we report a new computerized microfludic embryo culture and assay device which can perform automated periodic analysis of embryo metabolism over 18 hrs. The Microfluidic device is composed of a PDMS slab with microfluidic channel features (Figure IV. 1). Three separate channels (one has four branches for three samples including reference and a buffer; the others have single channel for introducing enzyme mixtures and substrate, respectively) converge into one single channel and divide into two branches. One is connected into a Buffer reservoir and the other is split into two different branches with its own reservoir, respectively: Sample Waste (BW) and Buffer Waste (BW). The three separate channels also have its own reservoir at the end of the channel in parallel. The first channel has a reservoir for enzyme mixture (HRP, GO). The middle channel has four separate branches with its own reservoir: sample 1(or culture media with single embryo), sample 2 (or culture media with sample multiple embryos), sample 3(or known Glucose concentration as reference). Third channel has a reservoir for substrate (Amplex red). In addition to a PDMS-parylene-PDMS hybrid membrane at the bottom, an Epoxy was coated on the surface of PDMS slab to keep media osmolality constant during measurements under non-humidified conditions.

The chip was placed on Braille-pin-based cell culture system by use of a monolithic and functional ‘‘fingerplate’’[24]. It precludes the need for chip removal/realignment to perform optical observations. The ability of dynamic microfluidic control (such as flow segmentation, multiple laminar flow generation, and mixing) is one of the common features of Braille-based microfluidic systems, and there is no change in the present microfluidic device that reduces these advantages. Figure IV. 1b shows the structure of a custom embryo culture/assay system. The system consists of four 2X4-pin Braille display modules, a

machined aluminum monolithic fingerplate with two hold-down clamps, a transparent heater unit. The monolithic fingerplate ensures stable chip mounting with sealing of the bottom membrane surface of the Braille-compatible PDMS microfluidic chip[25]. Four hold-down clamps are used to fix the microfluidic chip instead of rubber bands or weights used in the previous studies. Temperature is controlled by a digital temperature controller and a thermocouple glued to the surface of the slide glass. It heats only the cultivation of embryo in sample reservoir and reference reservoir to reduce degradation of enzyme and substrate.

We used a modified "Gated injection"[26] scheme to perform sample priming, reagent mixing, enzyme reaction (15 min) incubation, and sample detection as shown in figure IV. 2. First flow direction into both Buffer Reservoir (BR) and Buffer Waste (BW) was blocked by Braille pin valves and sample (or reference) and reagents are introduced from three reservoirs into a reaction channel using a pin actuation sequence for enhanced mixing[27] (Figure IV. 2b). After completion of priming, the mixed sample is incubated in a valve closed channel for 15 min to complete enzyme reactions. After 15 min, washing buffer in both BRs pushes the sample plug out through a detection zone where fluorescence intensity is measured and on to the BW. An automated program uses this gated injection scheme to sequentially measure fluorescence from sample, reference, and background (without any glucose) every hour for 18 hours.

In figure IV. 3, three different samples containing 100μM, 50μM and 25μM Glucose (Glucose Assay Kit, Molecular probes was used) and buffer (without any glucose) were loaded and their intensities were measured serially. After subtracting background, the intensity ratios of 25μM over 100μM and 50uM over 100uM are 0.26±0.01 and 0.43±0.01, respectively in figure IV. 3a. Because mechanical pumping and valves provided by Braille

pins movement are powerful and work firmly compared to eletrokinetic pumping and valve used in previous studies, the unwanted pressure driven backflow and resultant leakage can be dramatically overcome by our device. The low standard deviation over 18hrs demonstrates the accuracy and stability of this microfluidic analysis system. Standard curves with a wider range of glucose concentrations obtained from figure IV. 3a are shown in figure IV. 3b. The linearity of the assay at low levels of glucose (below 100μM) is well correlated that of the company provided protocol (Molecular probes).

Furthermore, this system was able to measure glucose consumption of single or multiple (10) live mouse embryos at the blastocyst stage. Approximate glucose consumption of embryos from the multiple and single embryos are 5pmol/hr per embryo and 13pmol/hr per embryo, respectively in figure IV. 4.

Conclusion

Appropriately designed enzyme assays can provide specific, precise, accurate, and reproducible estimates of levels of chemicals in solution. Microfluidic technology provides opportunities for integration and automation of such biochemical assays with microfluidic embryo culture. Conventional enzyme assay using the 96-well plate format, require a long assay time, use large quantities of sample and expensive reagents, and involve troublesome liquid-handling procedures. A microchip-based system overcomes these limitations and offers advantages such as enhanced reaction efficiency, simplified procedures, reduced assay time, and orders-of-magnitude reduction in consumption of samples and reagents[28].

This chapter reports real-time culture and analysis of single embryo metabolism using a microfluidic device with deformation-based actuation. Because mechanical pumps and valves actuated by Braille pin movement is powerful, unwanted pressure driven backflow and leakage is greatly reduced compared to electrokinetic fluidic schemes. The Braille-based actuation scheme also has an advantage that embryos are not exposed to any electrical field as would be required in electrokinetic schemes. The convenient, reliable, and automated nature of these assays also open the way for development of practical single embryo biochemical analysis systems for the IVF clinic.

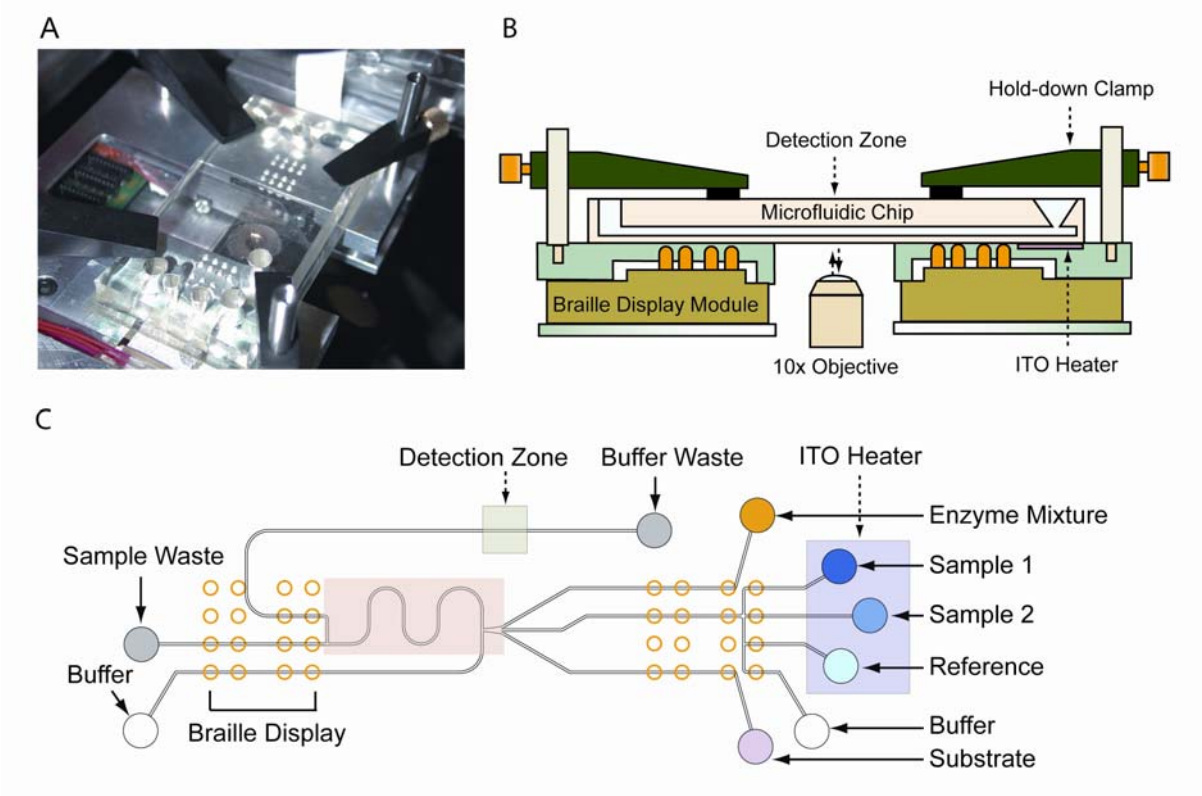

Figure IV.1. A portable Braille display-based microfluidic cell culture and assay system. The configuration of a PDMS microfluidic chip is installed on the Braille setup. The chip is fixed on a flat surface consisting of the fingerplate and the heater unit. The hold-down clamps are used to fix the chip by holding it down to the fingerplate. The Braille modules are fixed on the bottom plate so that the pins are aligned with the holes of the fingerplate. A. photograph of the whole system placed on a microscope system. B. Schematic cross-section of A. C. Schematic design of chip. ITO heater is attached on the Braille displayed module to keep the media temperature at 37°C for embryo survival.

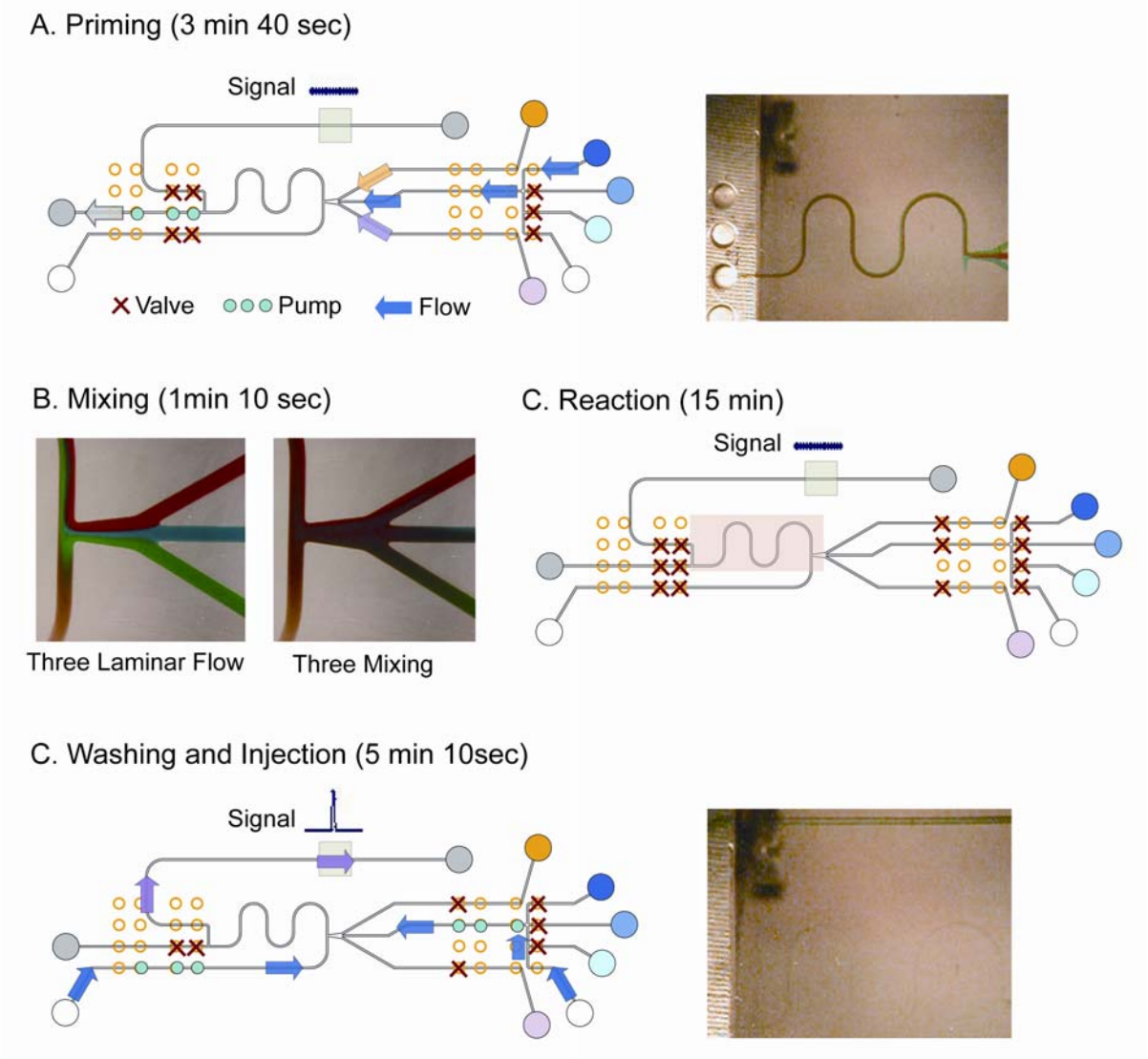

Figure IV.2. Modified "Gated injection": A. Sample priming, B. Mixing. Efficient mixing sequence performed by Braille pin movements. Three different flows are well mixed with the sequence (Right), while flow keeps laminar (Left) without the sequence. C. Enzyme Reaction (15 min). D. Sample Introduction into detection channel. Signal is detected at Detection zone. On each step, braille pins actuations for pumping and valve are controlled by programmed sequences on computer.

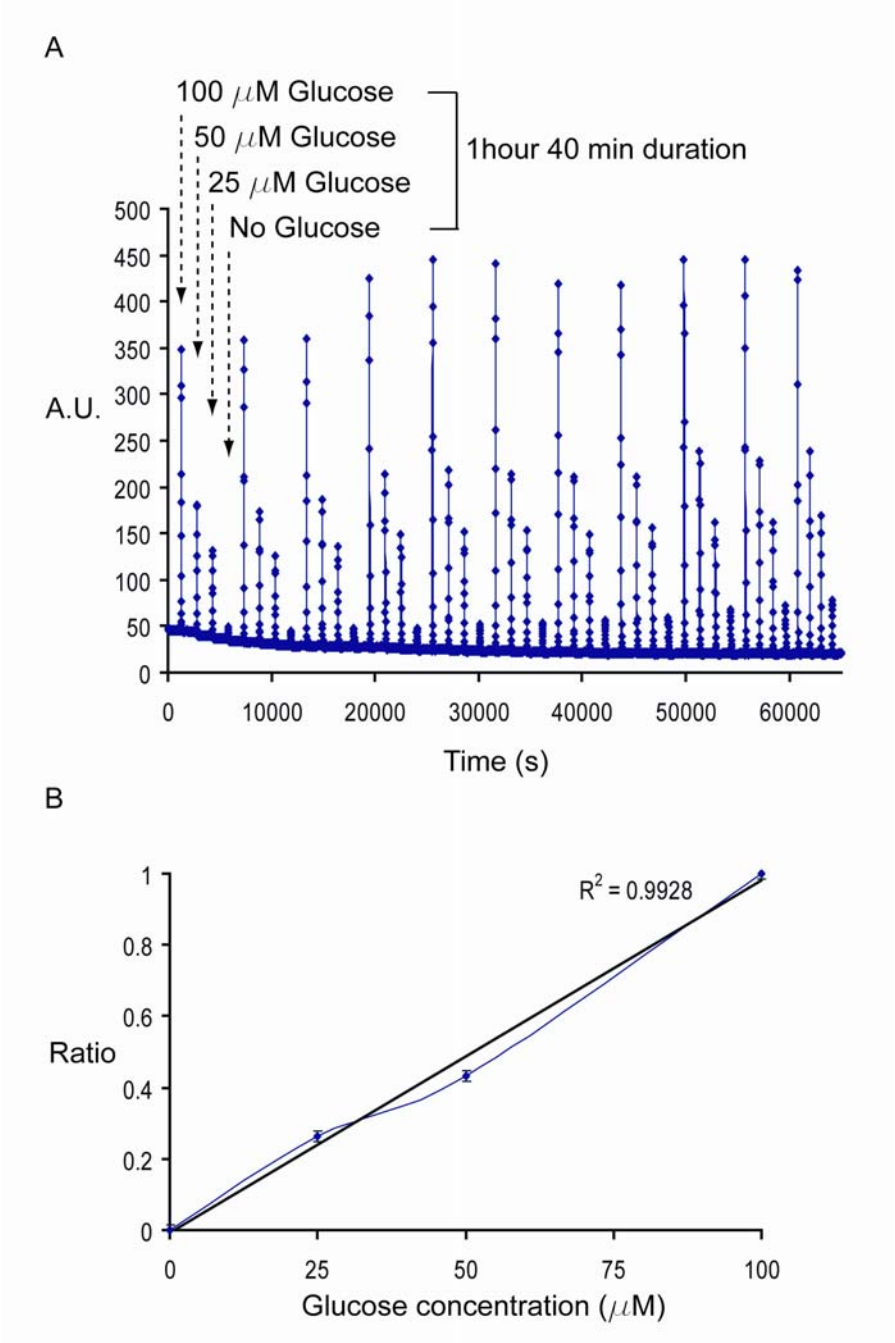

Figure IV.3. Glucose measurement on microfluidic devices. A. Each interval has a five second time lapse. 25μM, 50μM and 100μM Glucose concentration and background (No Glucose) were successfully measured over 18hrs. 4U/ml Glucose oxidase, 0.4U/ml Horseradish peroxidase as Enzyme mixture and 100μM Amplex Ultra Red as substrate were used. B. Standard curve with different concentration ratios from A.

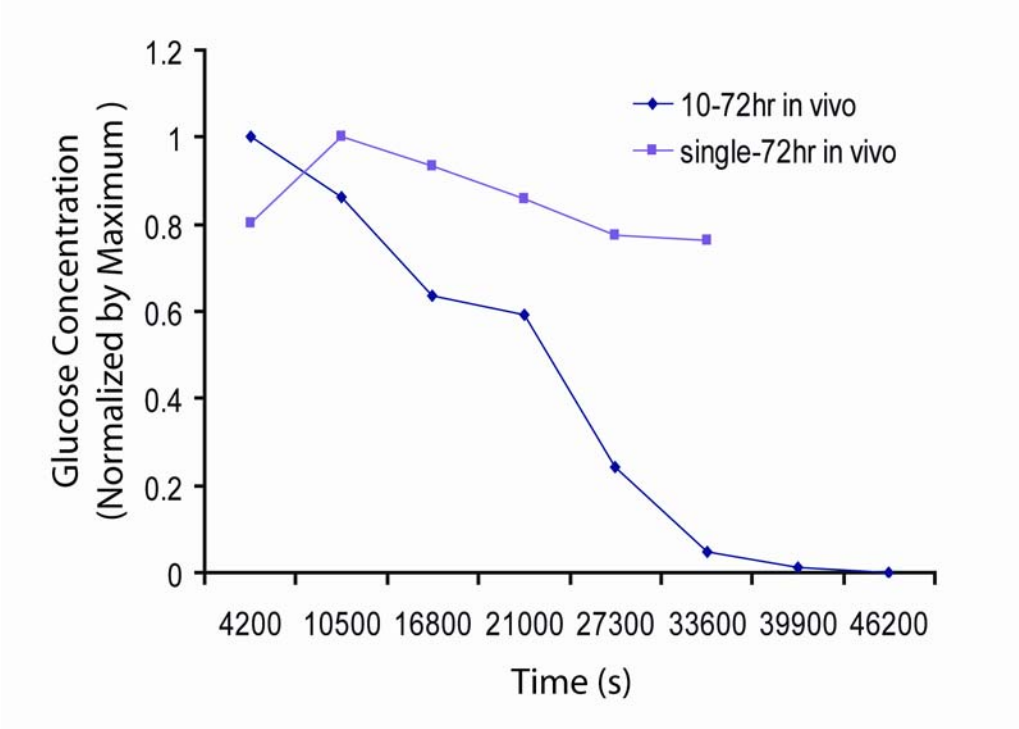

Figure IV.4. Glucose consumption of embryos. Both single blastocyst and multiple blastocysts (10) collected from B6C3F1 female mouse were culture and measured on chips over 10hrs. Approximate glucose consumption of embryos from 10-72hr in vivo and single embryo are 5pmol/hr/embryo and 13pmpl/hr/embryo, respectively.

References

[1] Wimalasundera, R. C., Trew, G. & Fisk, N. M. Reducing the incidence of twins and triplets, *Best Pract. Res. Clin. Obstet. Gynaecol.* **17** (2), 309 (2003).

[2] Cummins, J. M. *et al.* A Formula for Scoring Human Embryo Growth Rates in in-Vitro Fertilization Its Value in Predicting Pregnancy and in Comparison with Visual Estimates of Embryo Quality, *J. In. Vitro Fert. Embryo Transf.* **3** (5), 284 (1986).

[3] Shea, B. F. Evaluating the Bovine Embryo, *Theriogenology* **15** (1), 31 (1981).

[4] Lane, M. & Gardner, D. K. Selection of viable mouse blastocysts prior to transfer using a metabolic criterion, *Hum. Reprod.* **11** (9), 1975 (1996).

[5] Tesarik, J. & Greco, E. The probability of abnormal preimplantation development can be predicted by a single static observation on pronuclear stage morphology, *Hum. Reprod.* **14** (5), 1318 (1999).

[6] Van Royen, E. *et al.* Characterization of a top quality embryo, a step towards single-embryo transfer, *Hum. Reprod.* **14** (9), 2345 (1999).

[7] McKiernan, S. H. & Bavister, B. D. Timing of Development Is a Critical Parameter for Predicting Successful Embryogenesis, *Hum. Reprod.* **9** (11), 2123 (1994).

[8] Sher, G., Keskintepe, L., Nouriani, M., Roussev, R. & Batzofin, J. Expression of sHLA-G in supernatants of individually cultured 46-h embryos: a potentially valuable indicator of 'embryo competency' and lVF outcome, *Reprod. Biomed. Online* **9** (1), 74 (2004).

[9] Leese, H. J. What does an embryo need?, *Hum Fertil (Camb)* **6** (4), 180 (2003).

[10] Lopes, A. S., Greve, T. & Callesen, H. Quantification of embryo quality by respirometry, *Theriogenology* **67** (1), 21 (2007).

[11] Brison, D. R. *et al.* Identification of viable embryos in IVF by non-invasive measurement of amino acid turnover, *Hum. Reprod.* **19** (10), 2319 (2004).

[12] Houghton, F. D. *et al.* Non-invasive amino acid turnover predicts human embryo developmental capacity, *Hum. Reprod.* **17** (4), 999 (2002).

[13] Bromer, J. G. & Seli, E. Assessment of embryo viability in assisted reproductive technology: shortcomings of current approaches and the emerging role of metabolomics, *Curr. Opin. Obstet. Gynecol.* **20** (3), 234 (2008).

[14] Shoukir, Y., Chardonnens, D., Campana, A., Bischof, P. & Sakkas, D. The rate of development and time of transfer play different roles in influencing the viability of human blastocysts, *Hum. Reprod.* **13** (3), 676 (1998).

[15] Gardner, D. & Leese, H., *Assessment of embryo metabolism and viability. In Handbook of In Vitro Fertilization*, 2nd ed. (CRC press, Boca Raton, 1999).

[16] Gardner, D. K., Lane, M., Stevens, J. & Schoolcraft, W. B. Noninvasive assessment of human embryo nutrient consumption as a measure of developmental potential, *Fertil. Steril.* **76** (6), 1175 (2001).

[17] Hersen, P., McClean, M. N., Mahadevan, L. & Ramanathan, S. Signal processing by the HOG MAP kinase pathway, *Proceedings of the National Academy of Sciences of the United States of America* **105** (20), 7165 (2008).

[18] Li, P. C. H. & Harrison, D. J. Transport, manipulation, and reaction of biological cells on-chip using electrokinetic effects, *Analytical Chemistry* **69** (8), 1564 (1997).

[19] Burns, M. A. *et al.* An integrated nanoliter DNA analysis device, *Science* **282** (5388), 484 (1998).

[20] Duffy, D. C., McDonald, J. C., Schueller, O. J. A. & Whitesides, G. M. Rapid prototyping of microfluidic systems in poly(dimethylsiloxane), *Analytical Chemistry* **70** (23), 4974 (1998).

[21] Heo, Y. S. *et al.* Characterization and resolution of evaporation-mediated osmolality shifts that constrain microfluidic cell culture in poly(dimethylsiloxane) devices, *Analytical Chemistry* **79** (3), 1126 (2007).

[22] Futai, N., Gu, W. & Takayama, S. Rapid prototyping of microstructures with bell-shaped cross-sections and its application to deformation-based microfluidic valves, *Advanced Materials* **16** (15), 1320 (2004).

[23] Hogan, B., Beddington, R., Costantini, F. & Lacy, E., *Manipulating the Mouse Embryo*, 2nd ed. (Cold Spring Harbor Laboratory Press, Plainview, New York, 1994).

[24] Futai, N., Gu, W., Song, J. W. & Takayama, S. Handheld recirculation system and customized media for microfluidic cell culture, *Lab Chip* **6** (1), 149 (2006).

[25] Song, J. W. *et al.* Computer-controlled microcirculatory support system for endothelial cell culture and shearing, *Analytical Chemistry* **77** (13), 3993 (2005).

[26] Jacobson, S. C., Koutny, L. B., Hergenroder, R., Moore, A. W. & Ramsey, J. M. Microchip Capillary Electrophoresis with an Integrated Postcolumn Reactor, *Analytical Chemistry* **66** (20), 3472 (1994).

[27] Gu W, Zhu X, Futai N, Cho BS & S., T. Computerized microfluidic cell culture using elastomeric channels and Braille displays., *Proc Natl Acad Sci U S A.* **101** (45), 15861 (2004).

[28] Sato, K., Hibara, A., Tokeshi, M., Hisamoto, H. & Kitamori, T. Integration of chemical and biochemical analysis systems into a glass microchip, *Anal. Sci.* **19** (1), 15 (2003).

CHAPTER V

Conclusion

Development of *in vitro*-based systems that properly model the mechanical[1] and chemical[2] environments of embryos is necessary for advancing the understanding of IVF technologies and medicine. This dissertation research contributed to the field of IVF clinics by utilizing a microfluidic and microfabrication approach in improving upon the current state of the art of conventional *in vitro*-based systems[3,4]. Microfluidic systems provide the capabilities to properly mimic the mechanical and chemical environments which embryos encounter during development *in vivo*. 1 Herein we provide a framework for microfluidic embryo culture devices which show promise for basic biomedical research as well as IVF clinics. 2 Finally, since the described systems are rooted in microfabrication technology, we have established highly integrated systems that not only create more *in vivo*-like environments but can also further developed practical single embryo biochemical analysis systems for the IVF clinic.

In Chapter II, we provided a quantitative understanding of the relationship between evaporation and osmolality shift of cell culture media in microfluidic devices constructed of various thicknesses (0.1 to 10 mm) of PDMS and show how devices with thin PDMS layers lead rapidly to large osmolality shifts that result in cell death. Furthermore, we described methods to greatly suppress such osmolality shifts using

membranes with low water permeability and perform two biological demonstrations: 1. Static microfluidic culture of single cell embryos to blastocysts in submicroliter volumes of fluids over 4 days using a humidified incubator; and 2. Dynamic culture of primary human endothelial cells with recirculation of submicroliter volumes of media over 10 hours without media refreshment in a non-humidified environment. This study also provided a practical solution, PDMS-Parylene-PDMS "Hybrid" membrane for overcoming evaporation through thin PDMS membranes that is compatible with optical imaging as well as deformation-based microfluidic actuation. With this new insight and method, in chapter III we developed an *in vivo*-like microfluidic culture system with deformation based fluid actuation and successfully tested influences of microenvironment and dynamic media flow on embryo development.

In Chapter III, we reported a microfluidic based *in vivo*-like culture system used to close the gap between "in vivo" and current *In vitro* Fertilization (IVF). Compared to the *in vivo* cultured embryos, on-dish cultured embryos have many drawbacks: Lower embryo quality, implantation rates and fetus development rates *etc*. Recently, there have been studies on mouse embryo culture using dynamic environment microdevice but the results were poor compared with the static environment microdevice[5]. It is possible that these flow rates were still too high for mouse pre-implantation embryos, washing away necessary compounds in addition to waste products[6,7]. We thus hypothesized that what is necessary to better mimic the dynamic microenvironment that exists *in vivo* is to enable

physiological levels of fluid mechanical stimulation yet with retention of a significant portion of autocrine factors which are known to benefit embryo development[8]. Here we suggested a new computerized microfludic embryo culture device which can generate slower and pulsatile flow rates as well as provide fresh media continuously. This slow and pulsatile flow can provide an environment that is physically more similar to the *in vivo* reproductive tract environment (0.01~0.057 Hz in human uterus) and thus will be effective in increasing the current success rate of IVF (~ 30%). 1. embryo qualities (Numbers of Cells) were dramatically improved from Microdrop-control 67±3; Microfunnel-control 60±3 to Microfunnel-pulsatile 109±5 in microfluidic dynamic culture conditions. Blastocyst cell count following microfluidic dynamic culture more closely recapitulated results obtained from *in vivo*-grown blastocyst (144±9). 2. Importantly, the enhanced embryo development enabled by the dynamic microfunnel cultures led to correspondingly higher rates of implantation, lower rates of abortion, and significantly higher on-going pregnancy rates compared to embryos cultured in static microdrops ($P<0.05$). 3. Further, we studied an embryo's need for dynamic flow during development. We systematically varied the duration and developmental-stage at which embryos cultured in microfunnels were exposed to dynamic culture conditions and demonstrated that the number of cells is proportional to the number of times the embryo was applied with dynamic flow, irregardless of the order of static and dynamic condition. The system described in Chapter III marks a significant step in creating a microfluidic based platform capable of providing great insights into the mechanisms involved with dynamic environments *in vivo*. The user-friendly system architecture, flexibility in microchannel and chip design, and programmability of the fluid actuation system[9] allows

automated measurement of single embryo metabolism in Chapter IV as well as convenient and practical manipulation of chemical and mechanical microenvironment for *in vitro* embryo production in Chapter III.

In Chapter IV, we reported a new computerized microfludic real time embryo culture and assay device which can perform automated periodic analysis of embryo metabolism over 24 hrs. An automated program uses a modified "Gated injection" scheme (sample injection, reagent mixing, enzyme reaction (30 min) incubation, and sample detection) to sequentially measure fluorescence from sample, reference, and background (without any glucose) every hour for 24 hours. 1. The low standard deviation over 24hr demonstrates the accuracy and stability of this microfluidic analysis system. 2. Standard curves with a wider range of glucose concentrations were also obtained. 3. Furthermore, this system was able to measure glucose consumption of single or multiple (10) live mouse embryos at the blastocyst stage: 5pmol/hr per embryo and 13pmol/hr per embryo, respectively. Due to the powerful pumps and vales by Braille pin movement, unwanted pressure driven backflow and leakage is greatly reduced as well as embryos are not exposed to any electrical field as would be required in electrokinetic schemes. The convenient, reliable, and automated nature of these assays also open the way for development of practical single embryo biochemical analysis systems for the IVF clinic.

Collectively, the results presented in this dissertation confirm that microfluidic technology can be used to properly mimic a broad range of the in vivo environments seen in physiology that may govern embryo development. Microfluidic systems possess the

capabilities of precise fluid actuation[10], formation of independent cellular compartments for parallel experiments[11], and spatial control and delivery of biomolecules[12]. The work in this dissertation describes integration of these unique features of microfluidic systems and adapting them for embryo culture and analysis. By doing so, we establish that microfluidic systems have the capabilities of advancing IVF technology as it relates to embryo quality and pregnancy rates.

References

[1] Fauci, L. J. & Dillon, R. Biofluidmechanics of reproduction, *Annual Review of Fluid Mechanics* **38**, 371 (2006).

[2] Hardy, K. & Spanos, S. Growth factor expression and function in the human and mouse preimplantation embryo, *J. Endocrinol.* **172** (2), 221 (2002).

[3] Thompson, J. G. Culture without the petri-dish, *Theriogenology* **67** (1), 16 (2007).

[4] Trounson, A. O. & Gardner, D. K., *Handbook of in vitro fertilization* 2nd ed. (CRC Press LLC, Boca Raton, 2000).

[5] Hickman, D. L., Beebe, D. J., Rodriguez-Zas, S. L. & Wheeler, M. B. Comparison of static and dynamic medium environments for culturing of pre-implantation mouse embryos, *Comparative Medicine* **52** (2), 122 (2002).

[6] Paria, B. C. & Dey, S. K. Preimplantation embryo development in vitro: cooperative interactions among embryos and role of growth factors., *Proc Natl Acad Sci U S A.* **87** (12), 4756 (1990).

[7] Walker, G. M., Zeringue, H. C. & Beebe, D. J. Microenvironment design considerations for cellular scale studies, *Lab Chip* **4** (2), 91 (2004).

[8] Oneill, C. Evidence for the requirement of autocrine growth factors for development of mouse preimplantation embryos in vitro, *Biology of Reproduction* **56** (1), 229 (1997).

[9] Futai, N., Gu, W. & Takayama, S. Rapid prototyping of microstructures with bell-shaped cross-sections and its application to deformation-based microfluidic valves, *Advanced Materials* **16** (15), 1320 (2004).

[10] Unger, M. A., Chou, H. P., Thorsen, T., Scherer, A. & Quake, S. R. Monolithic microfabricated valves and pumps by multilayer soft lithography, *Science* **288** (5463), 113 (2000).

[11] Gu, W., Zhu, X. Y., Futai, N., Cho, B. S. & Takayama, S. Computerized microfluidic cell culture using elastomeric channels and Braille displays, *Proceedings of the National Academy of Sciences of the United States of America* **101** (45), 15861 (2004).

[12] Takayama, S. *et al.* Laminar flows - Subcellular positioning of small molecules, *Nature* **411** (6841), 1016 (2001).